NASA TECHNICAL
MEMORANDUM

NASA TM X-64599

A FINE SUN SENSOR FOR SKYLAB'S APOLLO TELESCOPE MOUNT

By J. D. Johnston
Astrionics Laboratory

March 31, 1971

NASA

George C. Marshall Space Flight Center

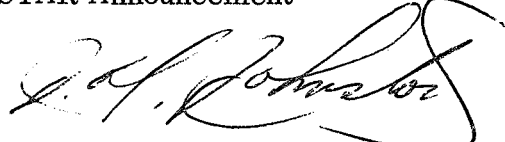*Marshall Space Flight Center, Alabama*

1. REPORT NO. NASA TM X-64599	2. GOVERNMENT ACCESSION NO.	3. RECIPIENT'S CATALOG NO.
4. TITLE AND SUBTITLE A Fine Sun Sensor for Skylab's Apollo Telescope Mount		5. REPORT DATE March 31, 1971
		6. PERFORMING ORGANIZATION CODE
7. AUTHOR (S) J. D. Johnston		8. PERFORMING ORGANIZATION REPORT #
9. PERFORMING ORGANIZATION NAME AND ADDRESS George C. Marshall Space Flight Center Marshall Space Flight Center, Alabama 35812		10. WORK UNIT NO.
		11. CONTRACT OR GRANT NO.
12. SPONSORING AGENCY NAME AND ADDRESS National Aeronautics and Space Administration Washington, D. C. 20546		13. TYPE OF REPORT & PERIOD COVERED Technical Memorandum
		14. SPONSORING AGENCY CODE

15. SUPPLEMENTARY NOTES

Prepared by Astrionics Laboratory, Science and Engineering

16. ABSTRACT

The three black boxes that make up the fine sun sensor assembly for the Apollo Telescope Mount are described. The performance characteristics, testing, and qualification results are also included. The design, evaluation, laboratory, and solar test results offer strong corroborative proof that such a system will give the Skylab a pointing capability of ±24 arc min in both pitch and yaw axes, accurate to 2 arc sec or less.

17. KEY WORDS Fine Sun Sensor Apollo Telescope Mount Skylab	18. DISTRIBUTION STATEMENT STAR Announcement

19. SECURITY CLASSIF. (of this report) Unclassified	20. SECURITY CLASSIF. (of this page) Unclassified	21. NO. OF PAGES 52	22. PRICE $3.00

MSFC - Form 3292 (May 1969)

TABLE OF CONTENTS

LIST OF ILLUSTRATIONS

LIST OF ILLUSTRATIONS (Concluded)

LIST OF TABLES

ACKNOWLEDGMENTS

A FINE SUN SENSOR FOR SKYLAB'S APOLLO TELESCOPE MOUNT

SUMMARY

This report contains the basic description of the three black boxes that make up the Apollo Telescope Mount (ATM) fine sun sensor (FSS) assembly. The performance characteristics, testing, and qualification results are also included. The design, evaluation, laboratory, and solar test results offer strong corroborative proof that such a system will give the Skylab a pointing capability of ±24 arc min in both pitch and yaw axes, accurate to 2 arc sec or less.

INTRODUCTION

The ATM-FSS (Fig. 1) provides two-axis attitude control with respect to the sun for the ATM. The ATM-FSS is activated after the ATM achieves orbit.

The ATM-FSS consists of an optical mechanical assembly, a pre-amplifier electronics assembly, and a control electronics assembly. As a system, the FSS provides two-axis attitude control and redundancy in each axis with respect to the sun for the Skylab's ATM.

The ATM-FSS is an extremely accurate sensor for determining the direction of the radiometric centroid of the sun. The system is pushing the state of the art for solar pointing accuracy and also for measurement techniques necessary to prove the sensor accuracy.

This report includes the ATM-FSS's basic design description and performance characteristics and also some typical test schemes and results from both Honeywell Radiation Center and NASA/MSFC.

DESCRIPTION

General

The ATM-FSS consists of an optical mechanical (OM) assembly, a preamplifier electronics (PE) assembly, and a control electronics (CE) assembly. The assemblies are located on the ATM as shown in Figure 2 with the OM and PE assemblies near the front relative to the sun. The integrated assemblies are shown in Figure 3. Physical size, power requirements, and temperature are contained in Table 1 and the interface requirements are contained in Table 2.

TABLE 1. ATM-FSS PHYSICAL CHARACTERISTICS

	OM	PE	CE
Weight (kg)	10.4	3.1	7.6
Size L×W×D (cm)	33×20.3×19	23.1×15×11.4	27.9×25.4×11.4
Volume (cm^3)	12,728	3966	8113
Unit Power Req. (W)			
Maximum Possible	13		7.5 Peak
Average	1	1	7
Dissipating Power (W)	800 mW (Two Motors)	1	7
Temperature (°C)			
Storage	10 +32	0 +35	-40 +54
Minimum Turn On	10	0	-40
Operational	10 +22	10 +22	-40 +47

TABLE 2. ATM-FSS ELECTRICAL INTERFACE REQUIREMENTS

FSS Inputs	
Spacecraft Power	28 ± 4Vdc 8 W, 126 ± 19 Vac, 400 Hz + 14%, 3W
Motor (Gimbal) Drive Command	0 to ± 5 Vdc
Primary/Redundant Command	+ 28 V Pulse
FSS Outputs	
Pitch-Yaw Error Signals	± 15 Vdc Max. (176 ± 32 mV/arc sec)
Sun Presence Signal	Switch Closure
Wedge (Gimbal) Readout	-2V to + 5V Pulse (1.25 arc sec)
Redundancy Status Signal	Open or + 28 Vdc
Test Point	J5 and J5 (PE and CE)

OM Assembly. The OM assembly (Fig. 4) contains four independent but functionally identical optical channels. Two channels (one primary and one redundant) are orientated for pitch sensitivity and two are orientated for yaw sensitivity. The OM assembly consists of three major subassemblies: the critical angle prism (CAP) base, fine wedge drive (FWD), and housing. The main structure for each subassembly (except for cases) is machined from a precedent 71A aluminum casting. The dimensions of the OM assembly are shown in Figure 5. This assembly weighs 10.4 kg.

The CAP base contains four prisms, choppers, and detectors; one for each channel. A flat is machined into the base to provide an external mirror to facilitate alignment to the ATM.

The prisms are kinematically mounted to the base on pads that are inserted into the base. Each prism is held against these pads by springs that are mounted in the clamping plates and the base casting. The plane of the three pads in front of the prism define the prism alignment; the pads are hand-lapped so that the prism is roughly aligned (30 arc sec) to the reference mirror.

The choppers and detectors are mounted directly behind the prisms. The detector is contained in a TO-5 can which in turn is cemented to a bracket to facilitate mounting.

FWD Assembly. The FWD assembly (Fig. 6) contains four deviation wedges, encoders, gear trains, and motors. The wedge, encoder pattern, detectors, helicon face gear, and wedge bearings for each channel are contained within a separate assembly as shown in Figure 7. The gear is pinned to the housing after initial adjustment for backlash. The code pattern is then installed and adjusted for concentricity to the rotating axis within ± 0.025 mm. The encoder detector assembly is then mounted to the bracket, attached to the housing, and shimmed so that the face of the detector is approximately 0.013 mm from the encoder pattern. Rotational adjustment of the detector assembly is accomplished by observing the encoder output when illuminated by a simulator and the encoder is rotated through 360 degrees. This assembly is then mounted to the drive mechanism (Fig. 8) and the gear is meshed to a backlash of less than 0.025 mm.

The motor and tachometer (Fig. 8) are a high reliability version of the Inland Type T-0709H dc torque motor. The motor has an output capability of 0.021 N-m when operated with the FSS electronics and a torque sensitivity of 0.0268 N-m/A. The brushes are made of a special material consisting of tantalum sintered with MOS_2 to enhance operation in vacuum. The tachometer has the same characteristics as the motor. The bearings for the motor shaft and pinion gear shaft are lubricated by duroid retainers. Both bearing sets are preloaded to approximately 0.9 kg by spring washers. The wedge assembly bearing is an angular contact bearing which is lubricated by a teflon wipe and teflon spacers. This bearing is preloaded to approximately 4.5 kg which is controlled by a machined spacer.

The helicon gear path has a speed reduction ratio of 71:1. Both gears are lubricated with MLR-2 solid lubricant (MOS_2 with an epoxy binder). The lubricant thickness is approximately 0.005 mm.

The motor shaft is attached to the pinion gear by a splined Rembrant coupling. The rotational play at the spline interface is less than 0.002 cm. The gears are meshed to a backlash of less than 0.002 cm at the mesh. This transfers through the optics to approximately 1.4 arc sec in deviation angle, which is the worst case anticipated.

The maximum torque output required from the motor is that required to overcome bearing, gear, and brush stictions and friction. Since inertia is low, and acceleration is not a requirement, these parameters can be neglected.

4

The output requirements for the motor under nominal operating conditions are summarized in Table 3.

TABLE 3. MOTOR OPERATING CONDITIONS

Motor breakaway torque (motor subassembly)	2.12×10^{-3} Nm
Pinion breakaway torque (helicon pinion — 2 pinion bearings — gear mesh — wedge bearing)	3.53×10^{-4} Nm
Minimum stall torque (amplifier saturated)	19.8×10^{-3} Nm
Factor of safety — $\dfrac{19.8 \times 10^{-3}}{2.5 \times 10^{-3}}$	8.0/1.0

The wedge drive assembly motors and detectors are wired to two connectors so that it may be operated as an independent subassembly. The subassembly is checked out before the complete assembly of the OM.

Once the CAP base and wedge drive assemblies have been completed, they are bolted together with the mounting feet on the drive assembly and holes in the CAP base. The housing, containing the alignment wedges and filter, is bolted to the base, and the connectors are installed. Then, the top of the wedge drive assembly is bolted to the walls of the housing to provide stiffening, and the cover is installed.

The assembly is then cycled through a series of vibration and temperature levels to relieve stresses that may have been introduced during assembly and submitted for final alignment by the alignment wedges.

The venting ports in the OM assembly allow back-filling with dry nitrogen during earthbound handling and test. They also allow evacuation during ascent. It should be noted that performance of the drive mechanism is degraded when operated in air because of the materials used.

Preamplifier Electronics and Control Electronics Assemblies. The ATM-FSS electronics are packaged in two separate assemblies, the preamplifier electronics assembly and the control electronics assembly.

The preamplifier electronics assembly (Fig. 9) is mounted directly behind the OM assembly and on spacers when installed in the spacecraft. The CE assembly is located on the rear bulkhead of the ATM canister.

The dimensions of the PE assembly are shown in Figure 10. This redundant assembly weighs 3.1 kg and contains 16 modules of electronics, 4 CAP preamplifiers, and 12 wedge readout amplifiers.

The CE assembly (Fig. 11) is also a redundant package and contains 16 modules of electronics, two 20-V power supplies, 4 motor drive circuits, 2 power supply regulator circuits, 2 power supplies, 2 clock generator circuits, and 4 control logic circuits. The dimensions of the CE assembly are shown in Figure 12. This assembly weighs 7.6 kg.

Each package consists of a precision cast mounting base and a precision cast U-shaped housing made of 356 aluminum, heat treated to the T-6 condition. The housing has two mounting rails, top and bottom, cast into three sides for mounting the electronics module boards. Each package has a top cover and a connector panel at one end, each containing five connectors (Cannon type PV7H) for signal input and output and for power and test.

The electronics are packaged using high density welded cordwood techniques. Each electronics module has an epoxy glass terminal board (a header) with bifurcated terminals that have a hole through the center of the terminal for attaching to the exit leads of the welded assembly prior to potting. The welded assemblies and attached header are potted with a rigid epoxy potting compound, MSFC 222 type 4. Each module has a minimum of two threaded standoffs swaged into the header for mounting. In the case of the motor drive and power supply modules, aluminum heat sinks have been designed to conduct the heat from the power diodes and transistors used in these circuits.

After potting, the modules are assembled to a black anodized aluminum plate with screws going into the threaded standoffs and/or the heat sink. The assembled module board is then assembled into the U-shaped housing by fastening it to the rails with screws. A wiring harness is then placed over the module board. The leads are soldered to each module and the harness is laced to small brackets located on the surface of the module board. The connector panel is then fastened to the main housing as well as the mounting base and the top cover.

Each assembly has a temperature sensing thermistor on the left side of the main housing between the two rails to facilitate monitoring internal temperatures through the assembly connectors.

Performance Characteristics

Performance characteristics of the ATM-FSS are contained in Table 4.

TABLE 4. ATM-FSS CHARACTERISTICS

Absolute Accuracy	2.25 arc sec
Pointing Resolution	± 0.625 arc sec (nominal)
Deviation Wedge Authority	± 24.21 arc min
Error Signal	176 ± 32 mV/arc sec
	(see Figs. 13 and 14)
Gimbal	
Readout	Incremental Serial Less Than 2 arc sec/s
Min Drive Rate	
Max Drive Rate	Greater than 80 arc sec/s
Drive Control	Open Loop, Manual

OPERATION

General

Since all four channels are identical, only one channel is described. Figure 15 shows a single channel of the ATM-FSS.

Sunlight passes through the alignment wedge which provides a spectral filter and a means for the final adjustment of a null axis relative to the external reference mirror. The sunlight then passes through the deviation wedge which refracts the sunlight at a fixed angle in a controllable direction. Direction control originates at the astronaut's hand control. This signal (0 to ± 5 V) is amplified by a dc torque amplifier which drives a dc motor. A comparator turn-on gate is included to reduce the gain of the amplifier when the motor has reached the desired mechanical position. When a signal input greater than 250 mV is applied, the gain of the amplifier is increased. The deviation wedge is rotated by the motor through a gear train, giving an apparent rotation of the

line-of-sight of the sun. Sunlight from the deviation wedge is then passed through the CAP. The CAP is a quartz prism whose isosceles angles are cut close to the critical internal reflectance angle for sunlight entering perpendicular to the front face. When light enters perpendicular to the base of the CAP, it is partially internally reflected. Of the remaining light, an equal amount passes through each face of the CAP and is focused on a detector. A chopper, at an 80-Hz rate, causes the detector to look alternately at the light from each face. If the angle of light incidence changes, more light passes through one side than the other. The output of the detector becomes a square wave with a peak-to-peak value proportional to the angular deviation of the incident light. This signal is amplified, demodulated, and sent to the ATM for position information. A sun-presence signal is also generated for the spacecraft.

Gimbal readout is accomplished by modulating sunlight with a three-track optical encoder that rotates with the deviation wedge. The encoder signal is detected, amplified, and sent to the ATM.

Detailed Operation

Optics. Sunlight passes through the alignment wedge and filter which provide a window, spectral filter, and a means for a final adjustment of a null axis relative to the external reference mirror. The ATM-FSS filter characteristics are shown in Figure 16. The sunlight then passes through the deviation wedge and the CAP.

The operation of the CAP is based upon the physical principle of total internal reflection. When light passes from a medium of higher index of refraction (N_2) to a medium of lower index of refraction (N_1), the transmission at the interface may be represented as shown in Figure 17 in which

$$\tau = 1 - \frac{1}{2}\frac{\tan^2(i-r)}{\tan^2(i+r)} + \frac{1}{2}\frac{\sin^2(i-r)}{\sin^2(i+r)} \quad ,$$

where

$\tau = \dfrac{I}{I_0}$, the ratio of transmitted to incident intensity

i = angle of incidence at the surface

r = angle of refraction, defined as $r = \sin^{-1}\left(n_2/n_1\right)\sin i$.

As angle i increases, τ decreases nonlinearly until sin i is equal to n_1/n_2 at which point the light is totally internally reflected and the transmission becomes zero (Fig. 18).

The formulation of the angle sensitive signal can be seen in Figure 19. Sunlight is incident on both inclined sides of the prism. If the sun center is in the null plane, sunlight strikes each side of the prism at the same angle. When the center of the sun is not in the null plane (Fig. 20), sunlight strikes side A at a larger angle of incidence than side B. Since the angle of incidence for side A has increased, the transmission has decreased and the flux magnitude in the transmitted beam has decreased, and conversely for side B. The result is a differential flux transmission through the two sides of the prism as a function of incident angle.

Figure 21 shows the simultaneous transmission of prism sides A and B as seen by the silicon detector. The difference in flux in the two beams is linearly proportional to the angle between the CAP's null plane and the sun radiometric centroid over a certain restricted angular region and restricted spectral passband. By detecting the flux differential, the error angle is effectively determined. The flux differentials between sides A and B are alternately chopped by a vibrating reed chopper and detected as shown in Figure 22.

By using a single detector, the CAP null is independent of detector responsivity or responsivity changes with time or ambient conditions. This is true because the flux bundles (a and b) strike the same area of the detector, and responsivity changes affect a and b uniformly. The CAP field of view (FOV) is controlled by the masking of the CAP and the location and size of the detector.

The critical dimensions (nominal) involved in the CAP design are illustrated in Figure 23. The following design criteria are exemplified:

- FOV limited to ± 1.5 degrees unvignetted (± 5.5 degrees max)

- Field stopping so that no stray light strikes the detector with less than two reflections

- Use of only one area of the detector for null sensing

- Approximately ± 30-percent tolerance for chopper blade excursion

- With chopper in the rest position (centered) the combined light from both sides is equal to that of either side at null giving the nominal ac-dc waveform characteristics.

<u>Chopper.</u> The chopper (Fig. 24) alternately interrupts, at an 80-Hz rate, the two beams of light that impinge on the photovoltaic cell located behind the CAP. The chopper has a thin reed of Nyspan C (a nickel-iron alloy) restrained at one end and free at the other. The chopper blade is mounted on the free end of the reed. The reed is mounted in a permanent magnet assembly consisting of two permanent magnets, two pole pieces, and two structures of soft iron. This assembly restrains the reed at one end and provides a magnetic field at the free end. When an alternating current is supplied to the drive windings, a magnetic field is induced at the ends of the Nyspan C. Depending upon the instantaneous polarity of the alternating current, the reed is deflected toward one pole piece and deflected from the other. The displacement of the reed is about ± 0.76 mm at 80 Hz during signal.

The chopper is driven so that the signals (Fig. 25) are flat on top. Variations in chopper amplitude do not change the magnitude of the square wave signals but increase or decrease the width of the flat portions.

The excitation voltage for the CAP's choppers is obtained by dividing the output of an 81.92-kHz clock by 512 to obtain 160 Hz. The 160-Hz output is divided by 2 to produce the 80-Hz excitation to a discrete component chopper drive circuit (Fig. 26).

<u>CAP Electronics.</u> The CAP electronics (Fig. 27) demodulate a dc/ac signal from the detector to provide a sun-presence indication and position information to the ATM control computer. The dc component is about 40 mV and is used to control an automatic gain control (AGC) circuit for the detector output. The ac component carries position information. The scale factor for this voltage is 0.064 mV/arc sec.

The AGC circuit consists of an integrated circuit amplifier (HY3) and an N-channel field effect transistor (FET) (Q1) across the output of the detector. The dc output of the detector is compared to a fixed reference (0.0402 V) at the input of HY3. Any input current over 4 μA is shunted through Q1 to ground, maintaining a predetermined dc level at the output of the detector.

When the sun is not present, the output of ac amplifier 1 (HY1) saturates transistor Q5. At this time, the gate to source voltage is well below pinch-off for Q2 and the output is zero. During sun presence, the output of HY1 cuts off Q5, allowing Q2 to conduct. Q2 then energizes a relay which gives the sun-presence indication.

10

For the sun-presence condition, HY1 has a 40-mV-dc input with an 80-Hz variable amplitude error signal. HY1 has a nominal gain of 248 V/V at 80 Hz. The output of HY1 is amplified by HY2 which has a gain of 6 V/V. The output of HY2 is then demodulated by two FET gates. Each FET gate alternately receives a 20-V, 1-ms sampling pulse that is time phased with the 80-Hz excitation but delayed about 3 ms. The sampling pulses are separated by 6.25 ms to provide phase discrimination. Each FET conducts only during the 1-ms sampling pulse, allowing a capacitor to be charged to the clamped input to the FET gate. The charge on the capacitor is amplified by a gain of 2 by HY4 and sent to the ATM control computer.

Because of the material selection for the chopper, the spring constant of the chopper blade gives rise to a highly underdamped system. Hence, the displacement of the blade is nearly in-phase with the excitation. Therefore, the control logic has been designed to generate the required 1-ms demodulator pulses to sample the chopper-generated error signals at the 90-degree point of the 80-Hz reference input.

Figure 28 shows the generation of the demodulator reference pulses. The 160-Hz input is divided down to 80 Hz in a flip-flop (HY1). At the same time, the 160 Hz is fed to a monostable multivibrator (HY2) which delays the 160 Hz for approximately 2.6 ms. The delayed 160 Hz is then inverted and again fed to a monostable multivibrator. The output of the second monostable multivibrator is a 1 ± 0.02-ms pulse at a 160-Hz rate. The 160-Hz, 1-ms pulses are "anded" with the 80-Hz, 0-degree pulses in HY5. At the output of HY4 are the required 80-Hz, 0- and 180-degree, 1-ms pulses shifted 90 degrees from the 80-Hz chopper input voltage.

The output pulses from HY4 feed discrete component demodulator drive circuits where the desired 20-Vdc level is obtained. The transistor output (Fig. 29) provides the synchronous 0- and 180-degree, 80-Hz + 20-Vdc demodulator reference drive signals for the CAP electronics amplifiers.

Clock Generator. The clock generator provides the basic clock reference for the system. The basic oscillator is a two-transistor circuit utilizing positive feedback (Fig. 30). The control of the oscillator frequency is based upon the piezoelectric effect of the crystal placed in the feedback path of an astable multivibrator.

The output of the oscillator is 0 to 6 Vdc in amplitude with an output impedance determined by the value of the collector resistance of Q2. Total operational power required is less then 5 mW.

The output of the crystal-controlled oscillator is fed to a divide-by-512 circuit. The division by 512 is accomplished using nine clocked flip-flops placed in series (essentially a 9-bit divider). The flip-flops are direct-coupled units operating on the "master-slave" principle. The clock input enters the master while the trigger input voltage is high and transfers to slave when the trigger input voltage becomes low. Since the operation depends only on voltage levels, rise and fall times of the input wave are not critical. The output of the clock generator is a 160-Hz square wave.

Encoder and Electronics. Each FWD contains a three-track optical encoder attached to the deviation wedge. As the wedge rotates, the encoder rotates with it (Fig. 31). .Sunlight that passes through the code wheel is detected by silicon photodiode detectors whose outputs are proportional to the amount of light impinging on them. Total angular motion is determined by counting the transitions from light to dark on the encoder (Fig. 32). The code segments are spaced according to an inverse sine relationship so that a feedback control system can be used to control the wedge speed to create a linear scan rate. Each code pattern also carries a zero-position reference mark. The zero-position mark is used to cage the wedge to the normal orient or zero position.

Outputs from the detectors are then fed to the wedge readout amplifiers. Those inputs are amplified by two differential amplifiers and a driver amplifier and sent to the astronaut's display.

Motor Control. The motor control input originates from a hand controller. Command input is 0 to ± 5 V (Fig. 33). This signal is fed to the integrated circuit amplifier HY1 and to a comparator turn-on gate made up of integrated circuit amplifiers HY2 and HY3.

To ensure that its motor cannot move when the desired mechanical position is obtained, the torque amplifier gain is reduced to a low gain condition. The gain is controlled by the comparator turn-on gate which operates as a function of input voltage. When the input voltage exceeds 250 mV in either division, a positive output is produced by either HY2 or HY3. This causes the 3N75 switch, Q7, to conduct, shorting out resistor R31. The output of HY1 is applied to transistors Q1 and Q2 for a positive output of HY1; transistor Q1 conducts which causes Q3 to conduct. This turns on Q4 which applies 20 V to the torque motor. For a negative output of HY1, Q2 conducts which causes Q5 to conduct. This turns on Q6, applying - 20 V to the torque motor. The ac feedback is supplied by C10, C11, and R26. The dc feedback is supplied by the tachometer and by the voltage developed across R30.

ATM-FSS Power Supply. The ATM-FSS power supply is a dc-to-dc converter operating from 28-Vdc power. It consists of an input filter, a 5-kHz oscillator, three isolated output voltage windings (20, -20, and 6 Vdc), and output filters. A ± 15-Vdc regulator is used with the power supply to provide supply voltage to the system electronics. The ± 20-Vdc power supply is used to drive the motors.

TESTING

General

The ATM-FSS was subjected to the tests described in the following paragraphs. Before starting and upon completion of each test, the temperature thermistor readings for the OM, PE, and CE assemblies were recorded; the solar intensity and the solar jitter (seeing condition) were also recorded. The pointing accuracy test mode is shown in Figure 34. Typical pointing accuracies and various drive rates for the ATM-FSS are shown in Figures 25 and 26, respectively.

Channel Alignment (Solar Test)

The OM assembly was mounted to the yaw holding fixture of the solar test stand and remained stationary during the test. The hour angle and declination tables were adjusted so that the OM was in the FOV of the sun. The "C" track of each channel was set to the zero reference position, using the hand-control input and the ATM-FSS monitor panel. The pitch axis CAP was set to the null position using the declination table. The hour angle table was rotated toward the west until the yaw channel CAP outputs were saturated. The primary and redundant CAP outputs were recorded as the sun scanned through the field. Multiple scans were made and recorded.

The declination angle (small angle) was decreased 24 ± 1 arc min and the test was repeated. The declination angle (null angle) was increased 24 ± 1 arc min above the original declination angle and the test was repeated.

The test procedure was then repeated with the pitch and yaw channels interchanged.

Pointing Accuracy (Solar)

The OM assembly was mounted to the yaw holding fixture of the solar test stand and remained stationary during this test. The hour angle and declination tables were adjusted so that the OM was in the FOV of the sun. The C track of each channel was set to the zero reference position using the hand-control input and ATM-FSS monitor panel. The pitch axis CAP was set to the null position using the declination table. The hour angle table was rotated toward the west until the yaw channel CAP outputs were saturated, and the CAP outputs were recorded as the sun scanned through the field. The yaw primary channel was tested first.

A positive hand-control input was then applied to the yaw primary wedge drive until the digital readout of the FSS monitor panel register changed from zero to a predetermined value (determined primarily on estimated available solar time) ranging from 1 to 1160 pulses. Theoretically, 1 pulse equals 1.25 arc sec and 1160 pulses equal 24.2 arc min. The pitch axis CAP outputs were set at the null position using the declination table. The hour angle table was rotated toward the west until the yaw channel CAP outputs were in saturation. The OM assembly was held stationary and the sun was allowed to scan completely through the FOV while the yaw channel CAP outputs and null crossovers were recorded on the recorder and computer. After multiple scans were obtained by repeating this process, multiples of the pulse number chosen were selected, and the procedure was repeated until the step function reached 1160 pulses. Next, a negative hand-control input was applied and the above test was repeated until the step function reached a negative 1160 pulses.

The test procedure was then repeated for the yaw redundant channel.

The OM assembly was then mounted to the pitch holding fixture of the solar test stand and the tests were run on the pitch primary and redundant channels.

Pointing Accuracy Test (Heliostat)

The OM assembly was mounted to the holding fixture of the precision turntable and the center of the heliostat reflection was pointed at the center plane of the four channels of the OM assembly. The C tracks of all four channels were set to the zero position using the hand-control input and the ATM-FSS monitor panel. The precision turntable was then adjusted for a null in the CAP output of each channel. The angle setting of the turntable was recorded. Each channel was subjected to the following test.

A positive input was applied to the wedge drive (using the hand controller) until the ATM-FSS monitor panel registered 1160 pulses. The remaining three channels were held at their zero reference positions and at CAP null. The CAP voltage was recorded and the turntable rotated until the channel was renulled. The change in the holding fixture angle was recorded. The procedure was repeated using a negative input.

The tests were then repeated using a number of pulses between 1 and 250 and were repeated using multiples of the number of pulses chosen until the step function reached 1160 pulses.

FOV Test (Heliostat)

The OM assembly was mounted to the holding fixture of the precision turntable and the center of the heliostat reflection was pointed at the center plane of the four channels of the OM assembly. The C tracks of all four channels were set to the zero position using the hand-control input and the ATM-FSS monitor panel. The precision turntable was then adjusted for a null in the CAP output of each channel. The angle setting of the turntable was recorded. Each channel was then subjected to the following test.

The turntable was rotated until the OM assembly reached a positive CAP saturation point. The angle change was recorded. The turntable was then rotated until the OM assembly passed through and started to drop out of positive saturation. The turntable continued rotating until the sun presence signal turned off, and then this angle was recorded. The turntable was rotated until the channel reached its FOV limits. This angle was also recorded.

Substituting the word "negative" for the word "positive" in the previous paragraph, the same test was repeated for the negative side of the FOV test.

FSS Qualification

Only the summary results of the qualification tests conducted on the ATM-FSS are included in this report. For more detailed information refer to the "Qualification Test Report of the ATM Fine Sun Sensor (21001918) for Use on the Apollo Telescope Mount, Contract No. NAS8-20733." This report was prepared for MSFC by Honeywell Radiation Center. A 100-day test was performed to determine the performance of the motor and gear train of the wedge drive assembly. This test and the results are contained in Appendix A of the above-mentioned report.

Applicable Documents. The qualification tests were conducted according to the following documents:

1. MSFC documents

   a. 50M02408B — Environmental Design and Qualification Test Criteria for Apollo Telescope Mount Components

   b. 50M02407 — Test Program Guidelines for Apollo Telescope Mount

   c. 50M12725 — Electromagnetic Compatibility Control Plan for ATM.

2. Government documents

   a. MIL-I-6181D — Interference Control Requirements

   b. MIL-E-6051C — Electronic System Compatibility and Interface Control Requirements

   c. MIL-B-5087B — Electrical Bonding for Aerospace Systems.

3. Honeywell test documents

   a. ATP 1001 (21001867)   Preamplifier Electronics Acceptance Test Procedure

   b. ATP 1002 (21001869)   Control Electronics Acceptance Test Procedure

c. ATP 1003 (21001868) Optical-Mechanical Acceptance Test Procedure

d. ATP 1004 Fine Sun Sensor System Acceptance Test Procedure

e. EEP-2206 Evaluation Engineering Specification for Qualification Tests of the ATM-Fine Sun Sensor System.

4. Honeywell drawings

a. 21001868 — Optical Mechanical Assembly

b. 21001867 — Preamplifier Electronics Assembly

c. 21001869 — Control Electronics Assembly

d. 21001918 — ATM-FSS Subsystem.

Test Plan. The tests were conducted at the following two levels:

1. Subsystem level — where each of the three major subassemblies was tested as a discrete component.

2. System level — where the three assemblies were interconnected and operated as a system.

The ATM-FSS was subjected to a series of test at the acceptance test level before submission to the Qualification Test Program. Figure 37 illustrates the qualification test flow of the ATM-FSS.

Test Results. Qualification tests were conducted on the FSS system, serial number 001, during the calendar period of 8-20-69 through 2-28-71. During this period the system and/or the subsystems were subjected to various environmental exposures with a series of pre- and post-exposure testing.

The results of these test have resulted in some corrective changes along the way, but only to give assurance to a more accurate and reliable system.

CONCLUSIONS

The design and test evaluation has proven that in a properly controlled environment, such as the packed ATM experiment will have, the Skylab's ATM-FSS is capable of pointing the ATM experiment package to within 2.25 arc sec of the radiometric center of the sun; it also provides a ±24 arc min pointing capability from the sun centroid in both pitch and yaw axes, accurate to 2.25 arc sec or less.
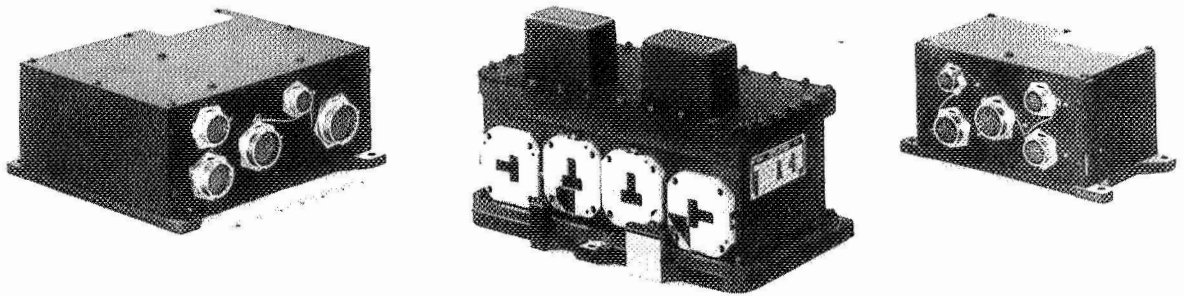
Figure 1. ATM-FSS.
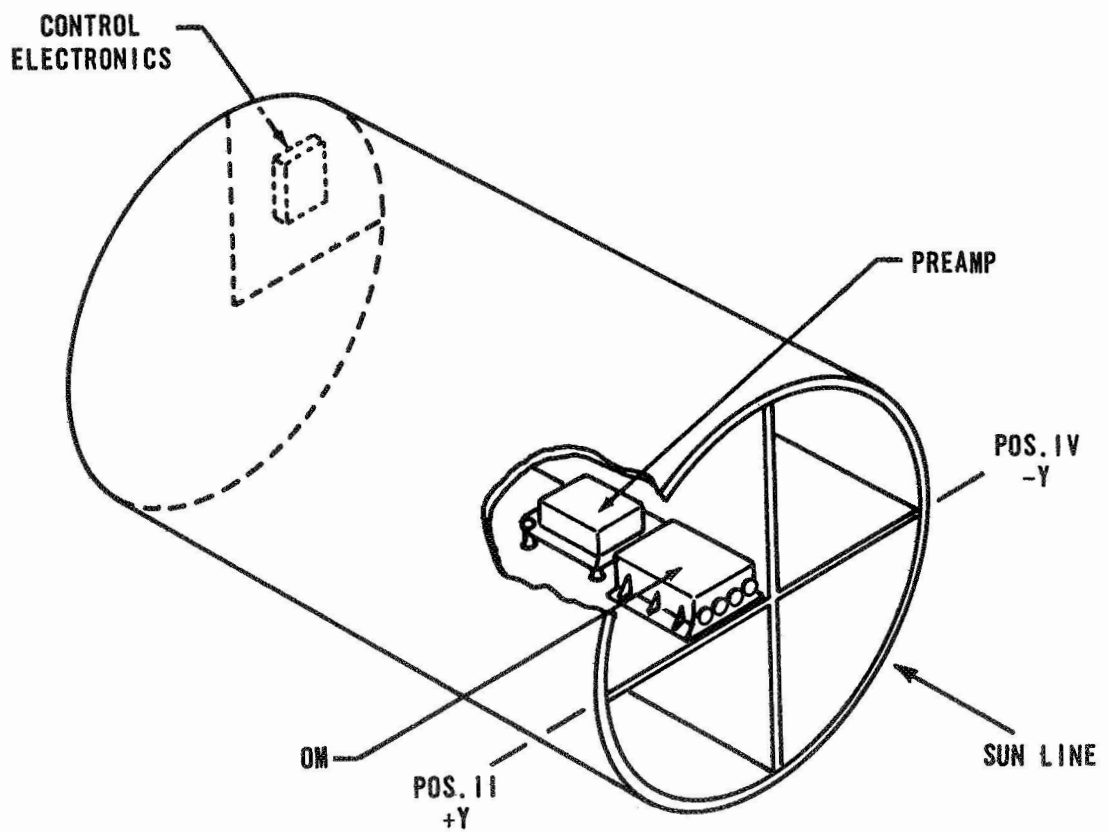
Figure 2. ATM-FSS component location on the ATM.
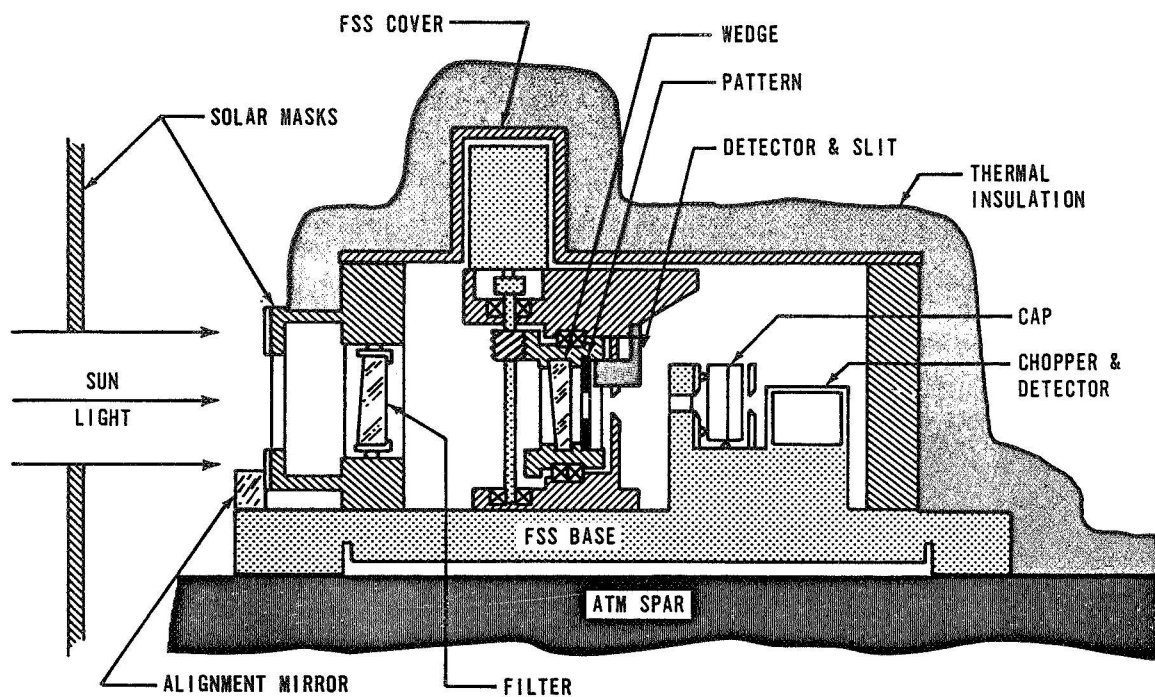
Figure 3. Integrated assemblies.
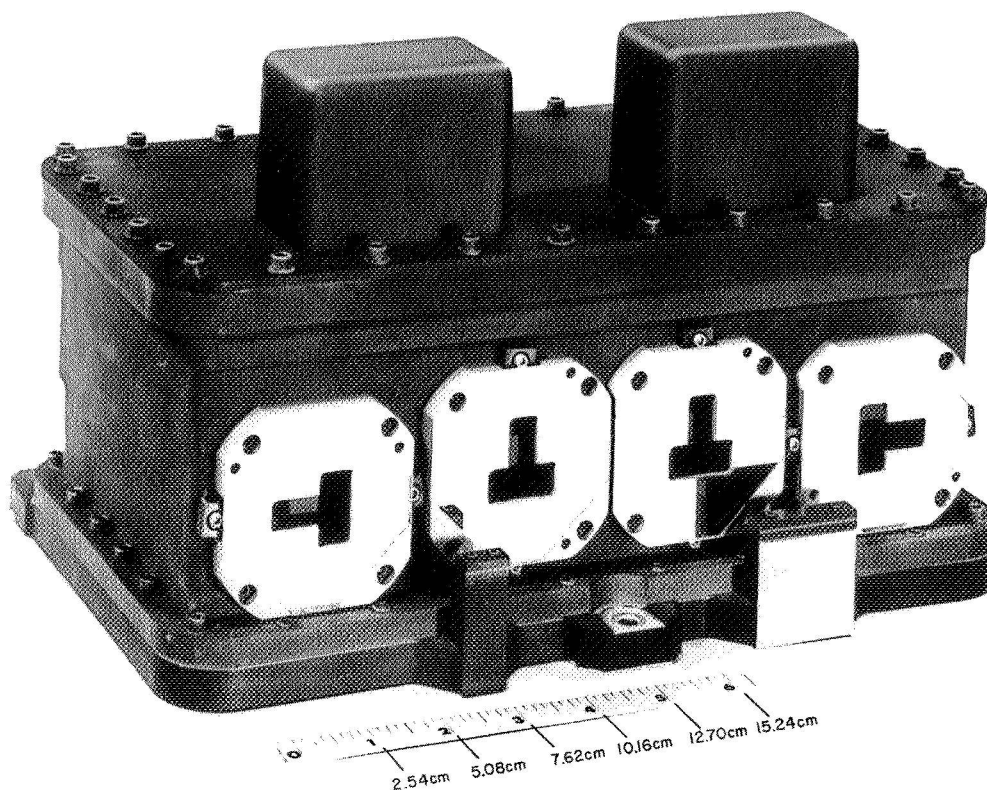
Figure 4. OM assembly.
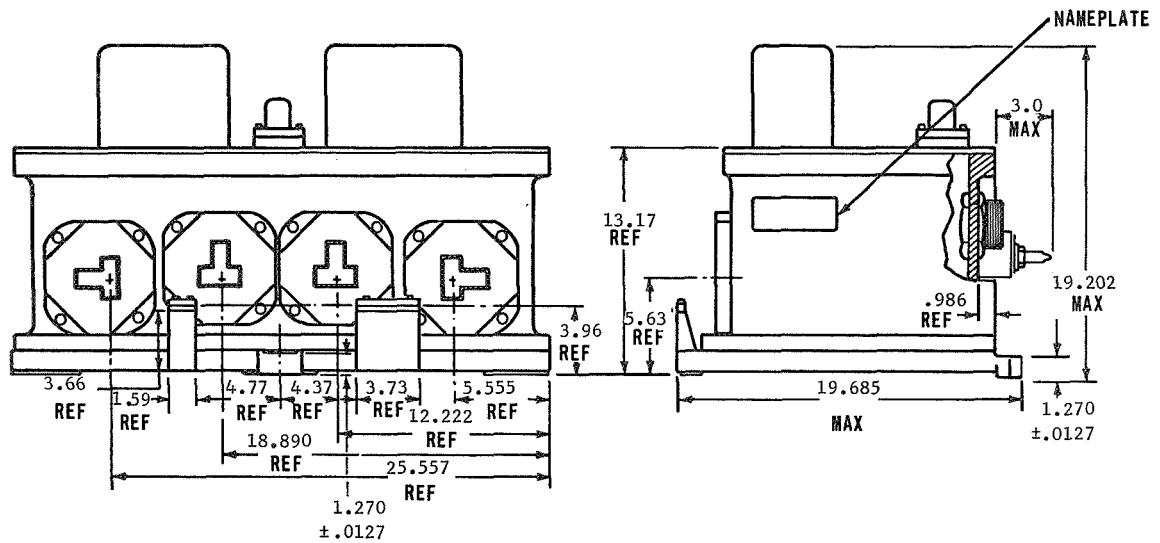
Figure 5. OM assembly dimensions.
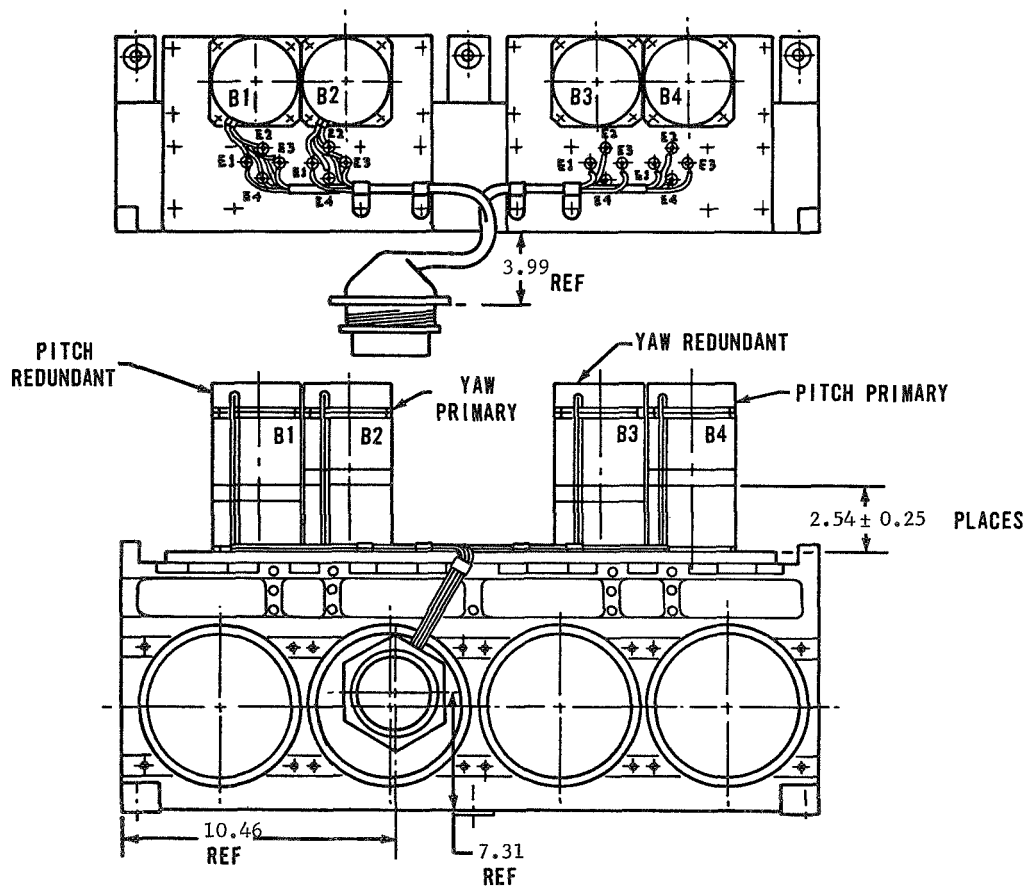
Figure 6. FWD assembly dimensions.

PIN

WEDGE BEARING

HELICON
GEAR

DETECTOR
ASSEMBLY

WEDGE
RETAINER

CODE
PATTERN

PATTERN
RETAINER

DEVIATION
WEDGE

E1 E3 E4 E6
E2   E5

PITCH 21000122-101
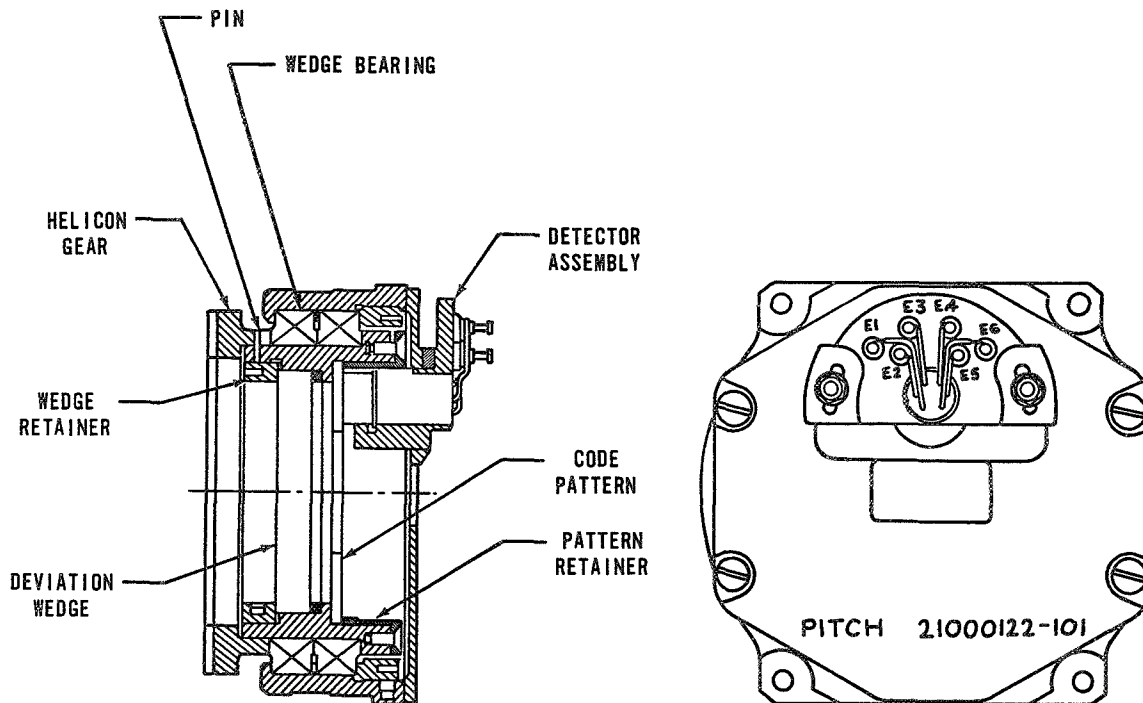
Figure 7. Deviation wedge and encoder assembly.

MOTOR
& TRACK ASSEMBLY

CASTING

SPLINED COUPLING

PIN

PINION BEARINGS
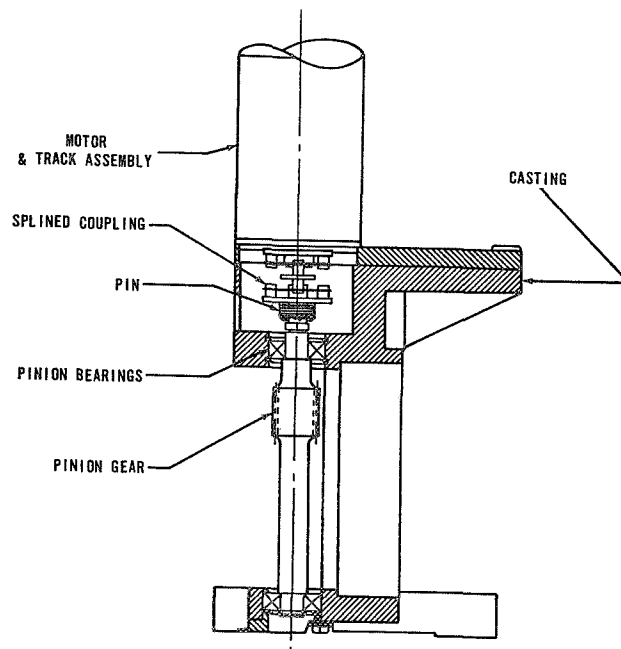
PINION GEAR

Figure 8. Motor and pinion gear drive mechanism.
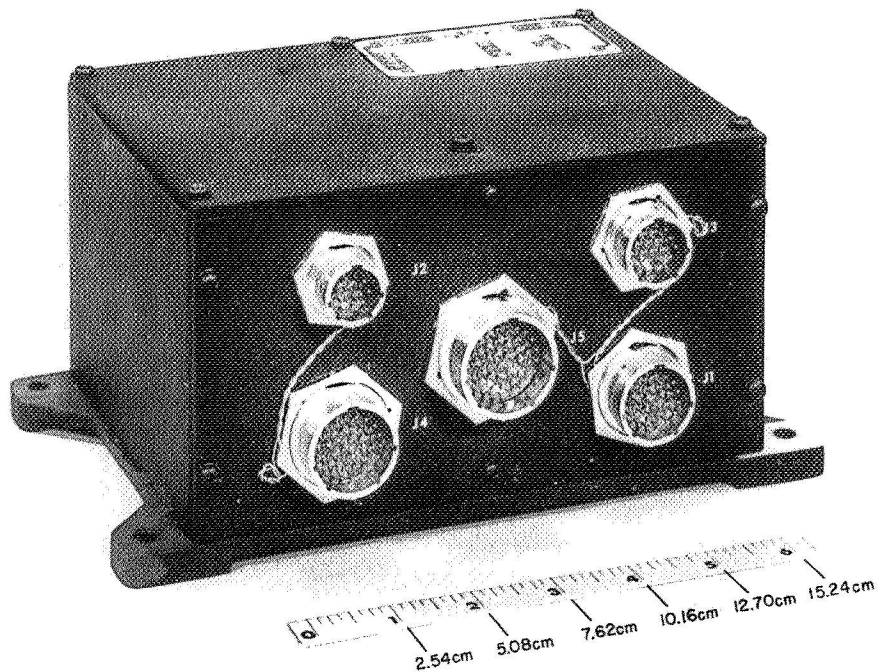
Figure 9. Preamplifier electronics assembly.
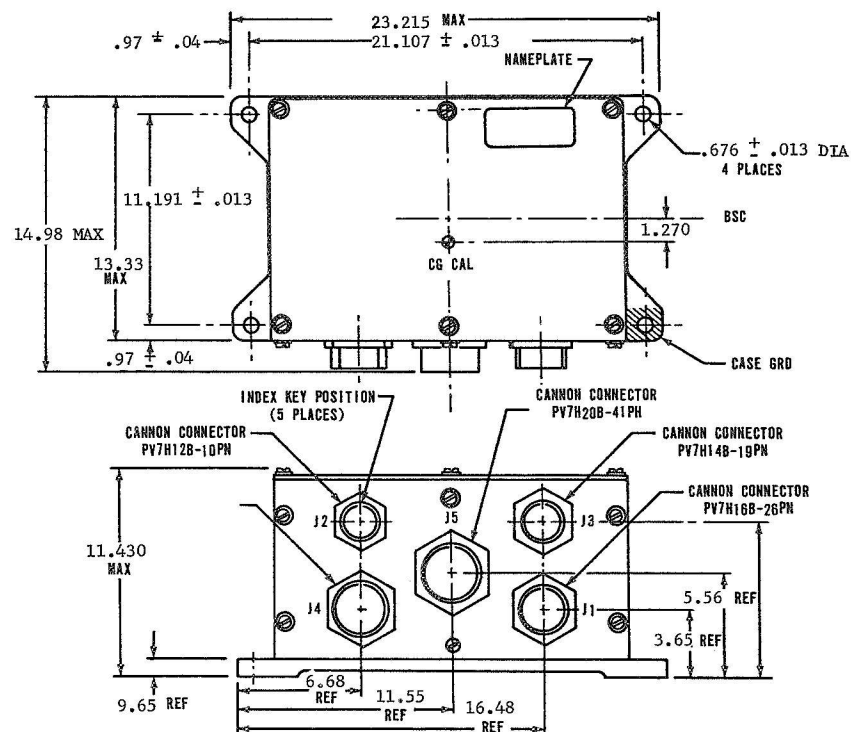
Figure 10. PE assembly dimensions.
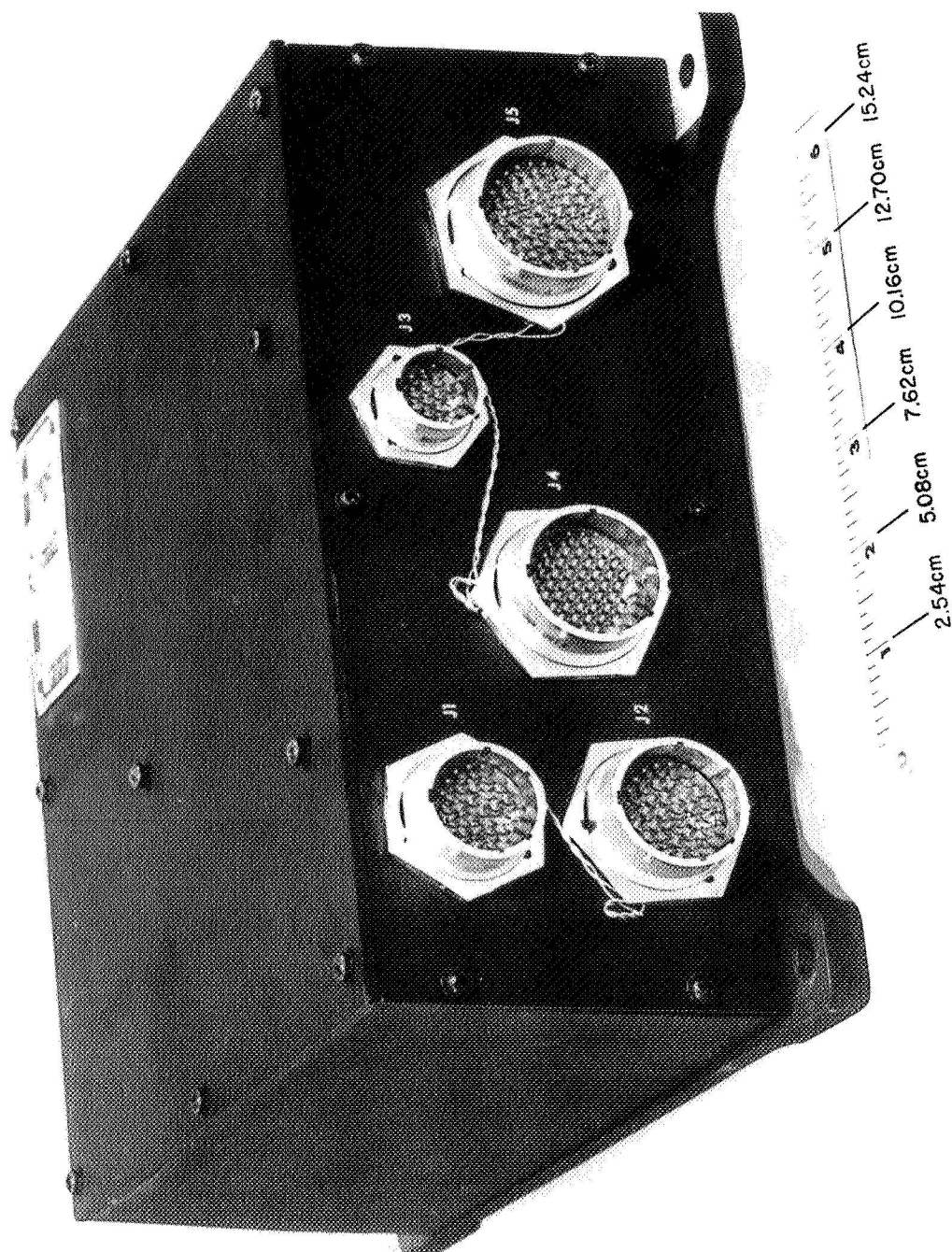
Figure 11. CE assembly.
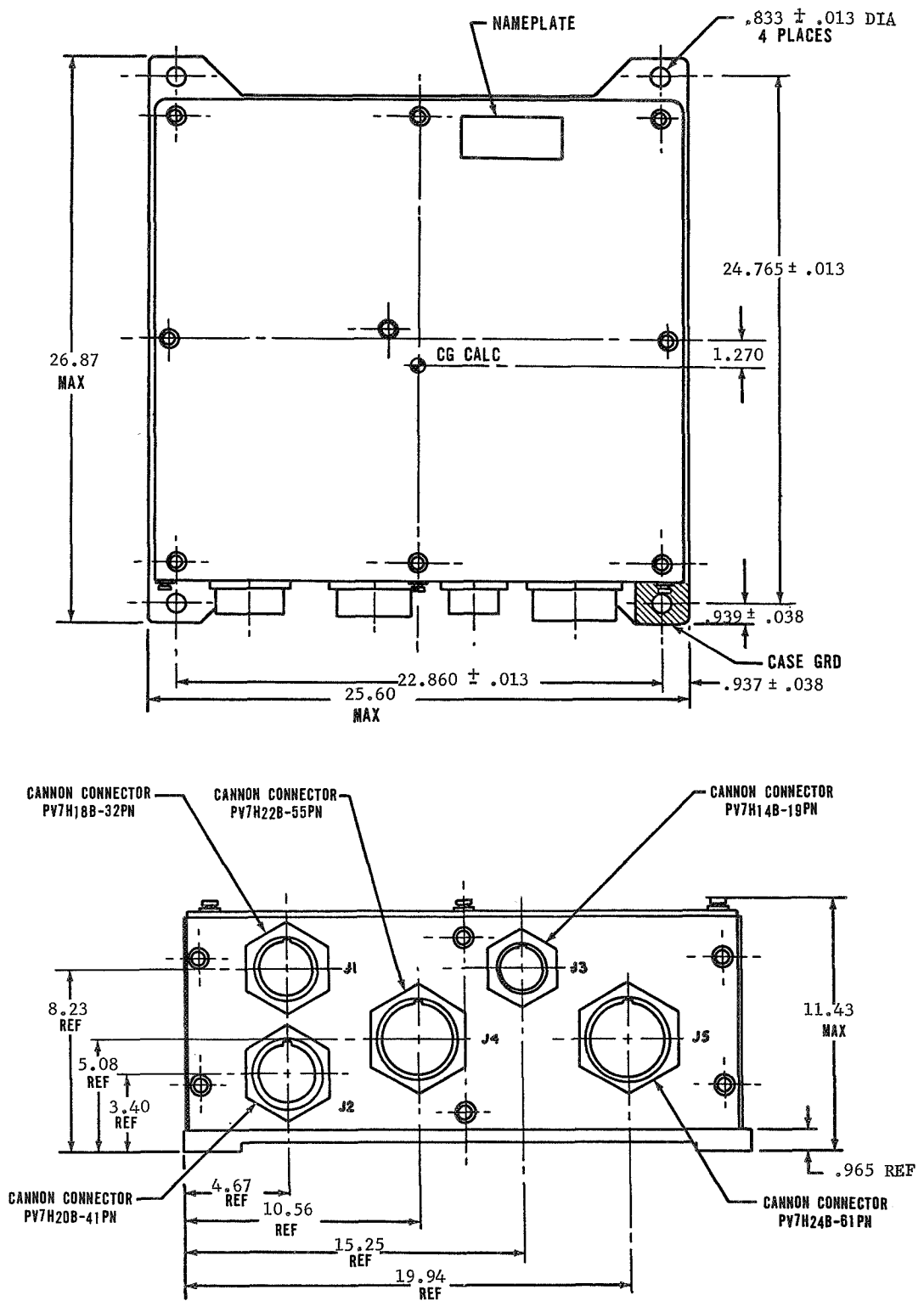
Figure 12. CE assembly dimensions.
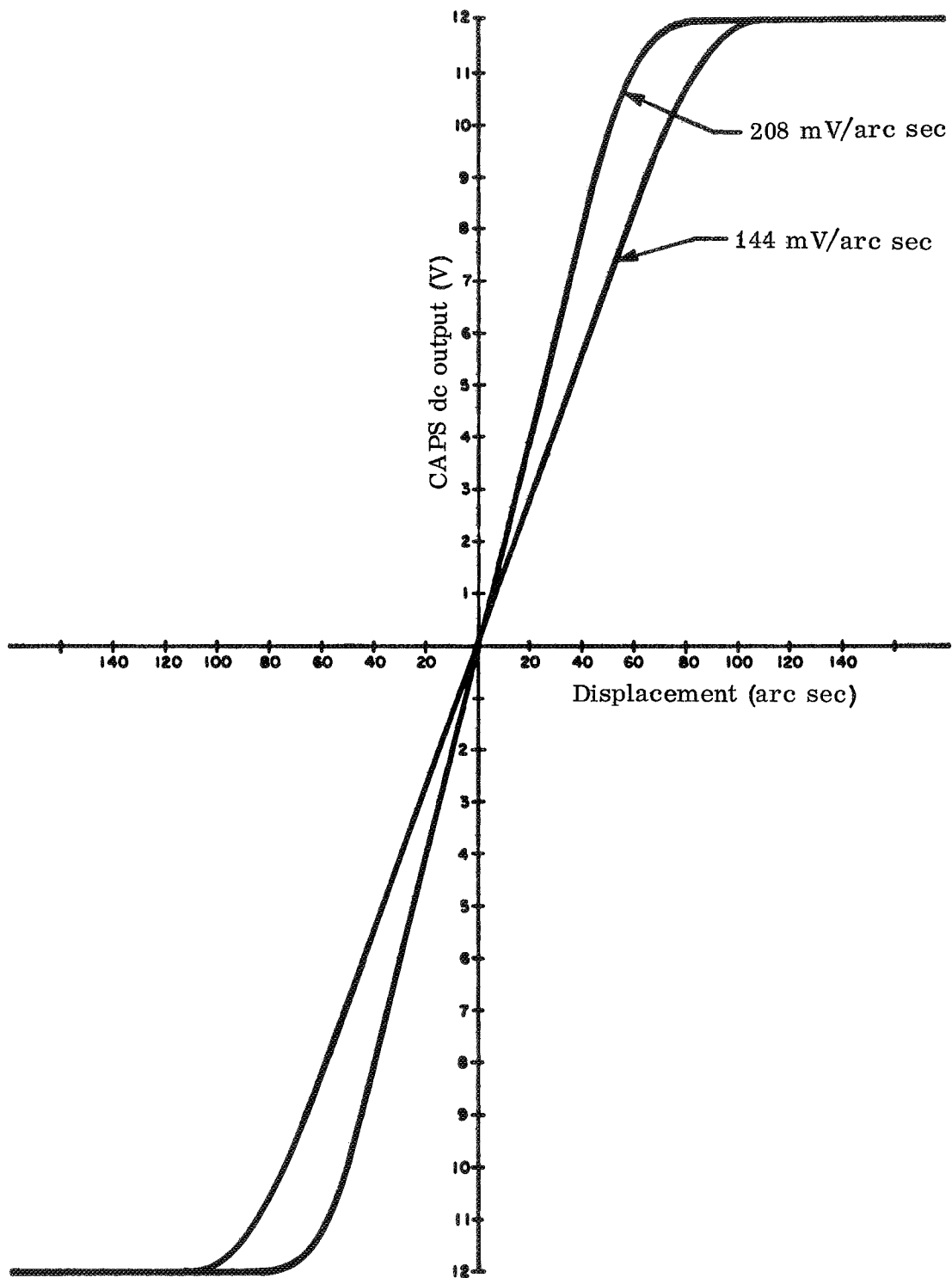
Figure 13. ATM-FSS CAP dc output about null.
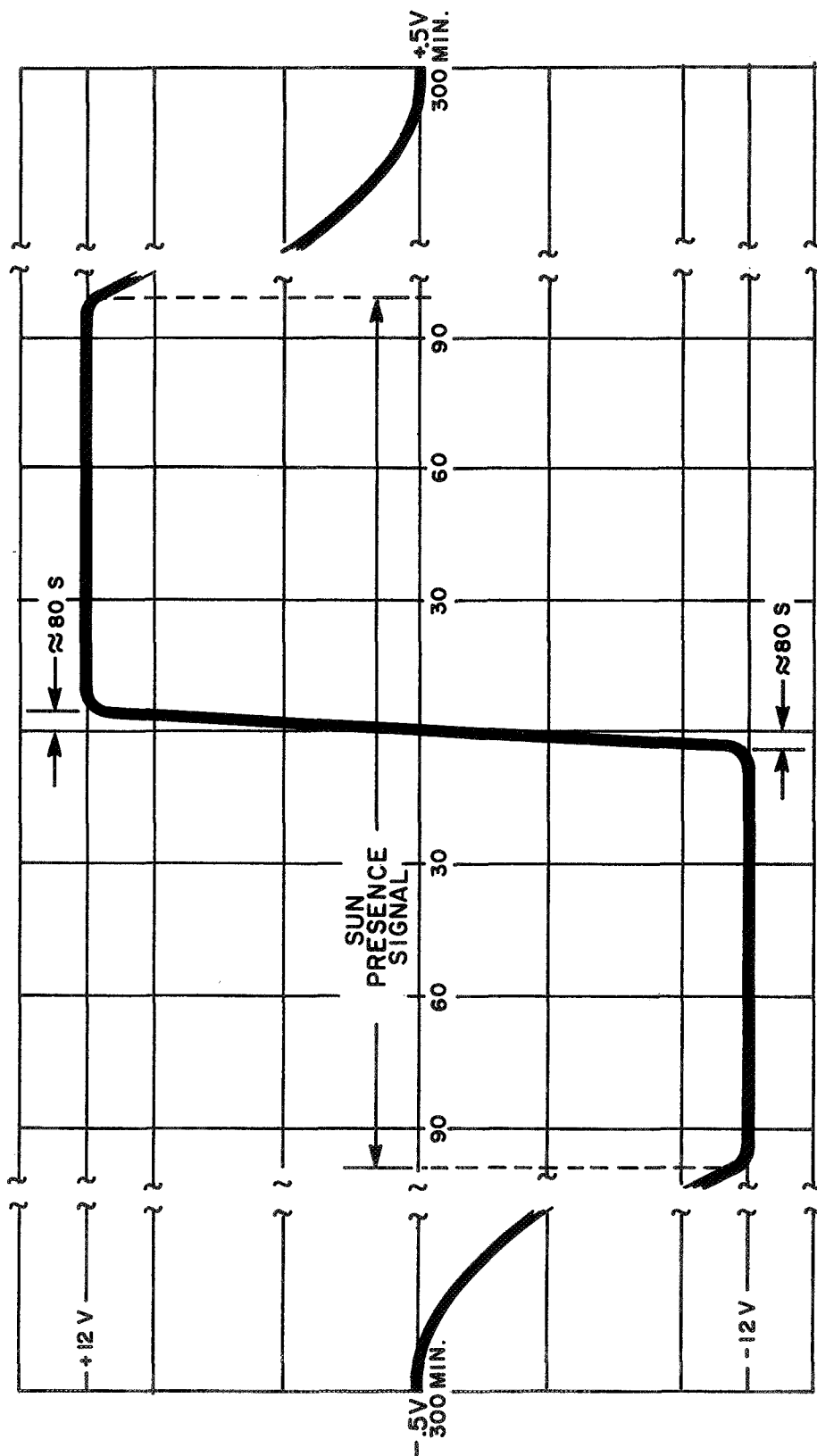
Figure 14.   ATM–FSS field–of–view output relationships — Typical curve.

27
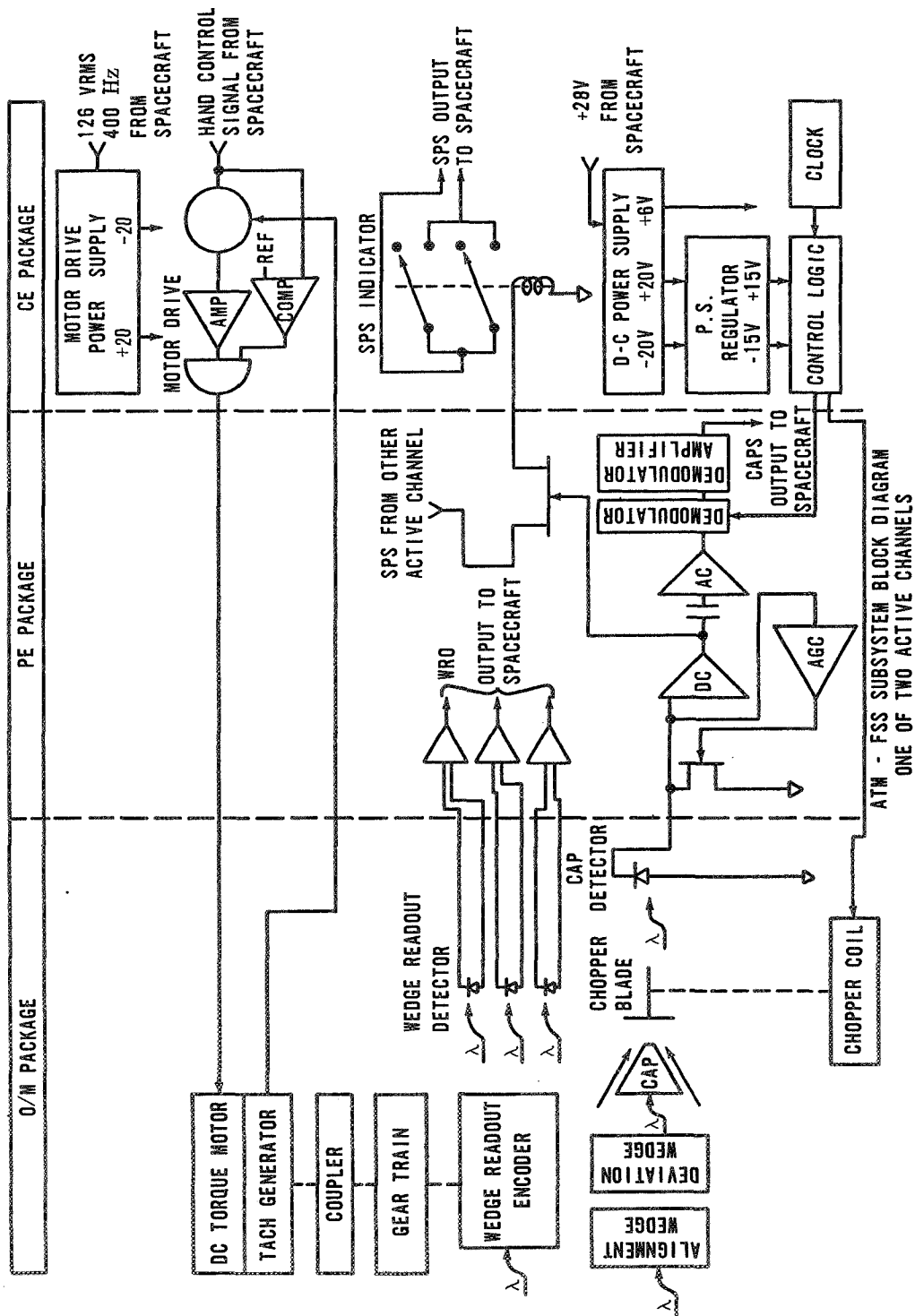
Figure 15. ATM–FSS block diagram.

28
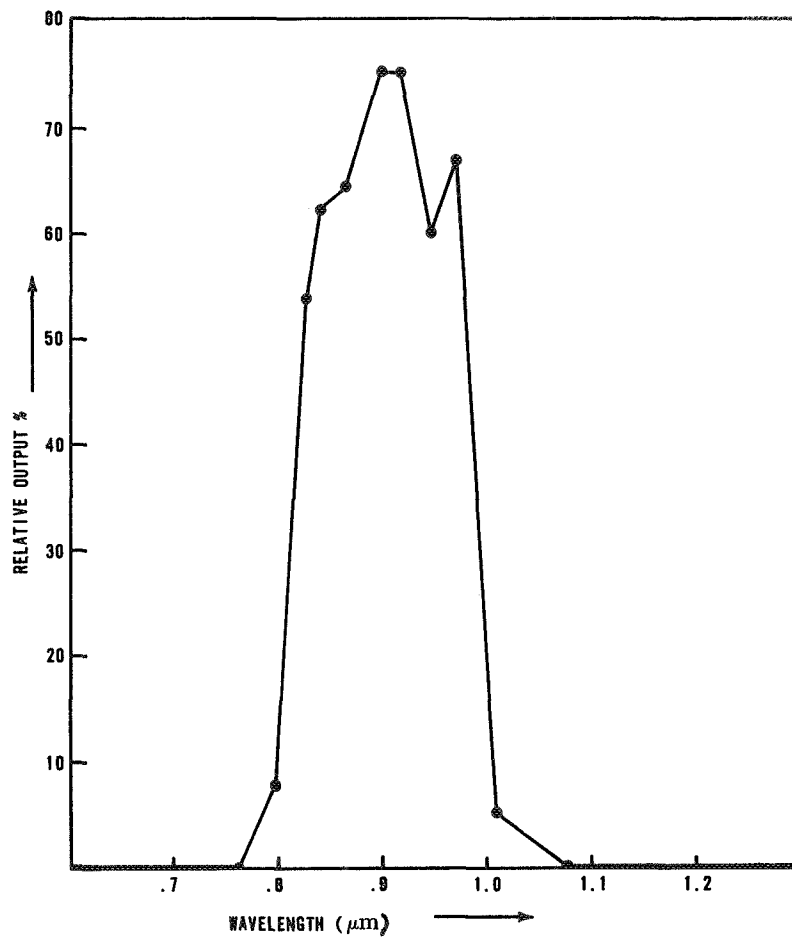
Figure 16. ATM-FSS filter transmission characteristics.
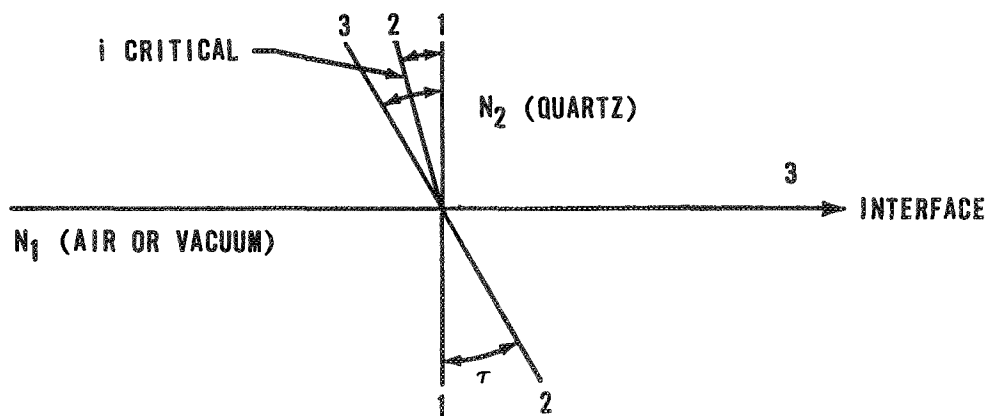
Figure 17. Transmission at interface.

QUARTZ ($\eta = 1.452$)
TO $\eta = 1.0$

ANGLE OF INCIDENCE (1)
(DEGREES)
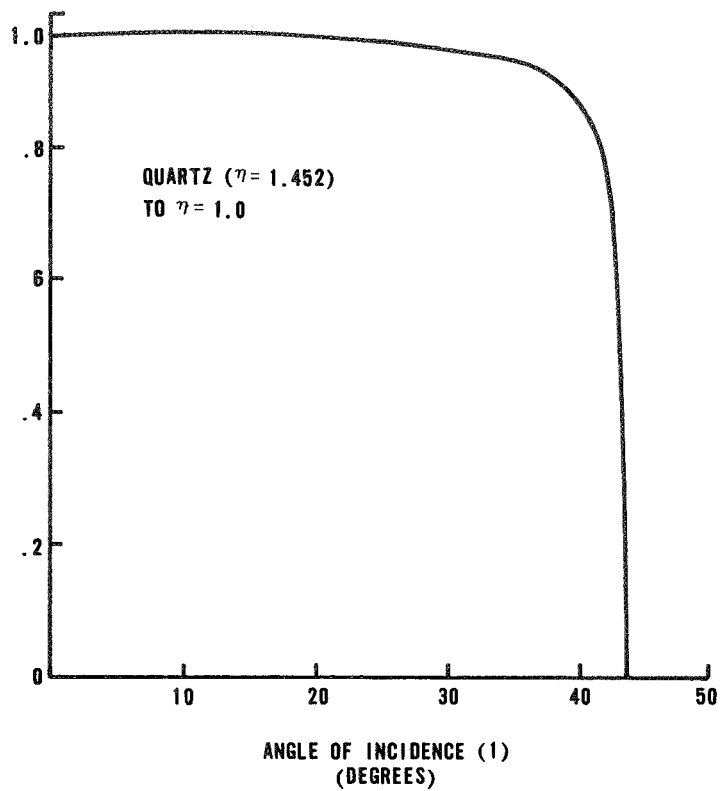
Figure 18. Point of total internal reflection.

INCIDENT SUNLIGHT

SIDE A

SIDE B

TRANSMITTED BEAM
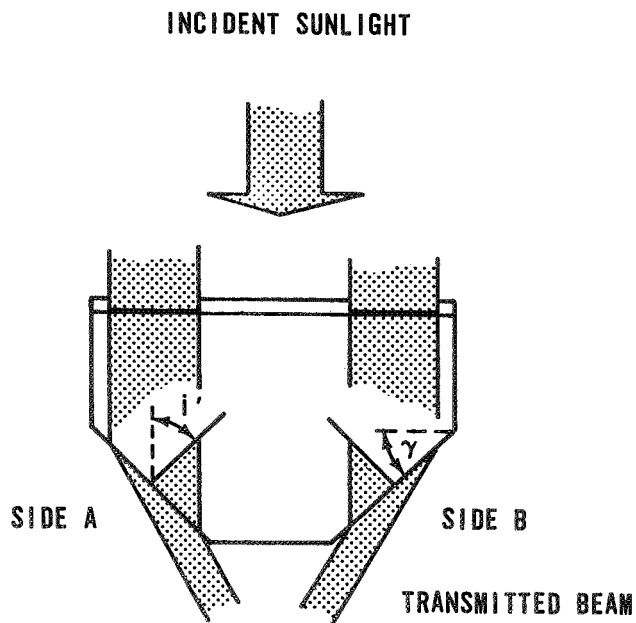
Figure 19. Prism transmission with sun on axis.
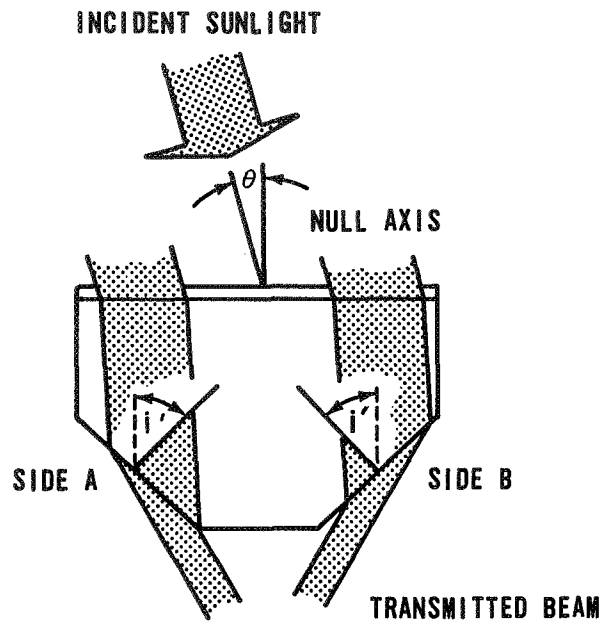
Figure 20. Prism transmission with sun off axis.
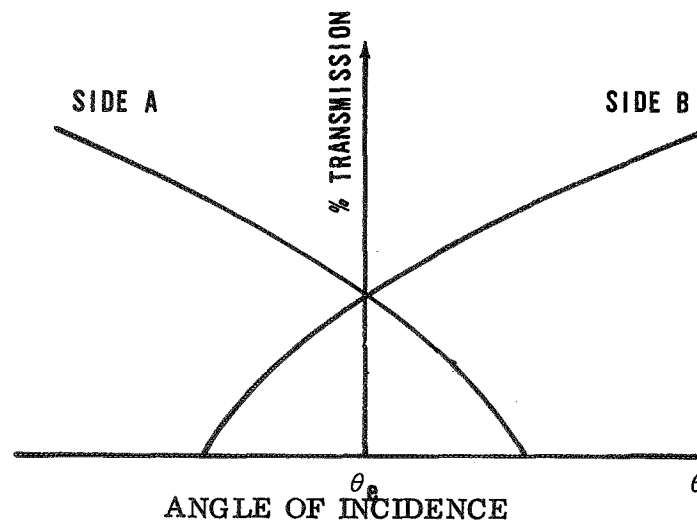
Figure 21. Light transmission through the prism.

INCIDENT SUNLIGHT

CHOPPER BLADE
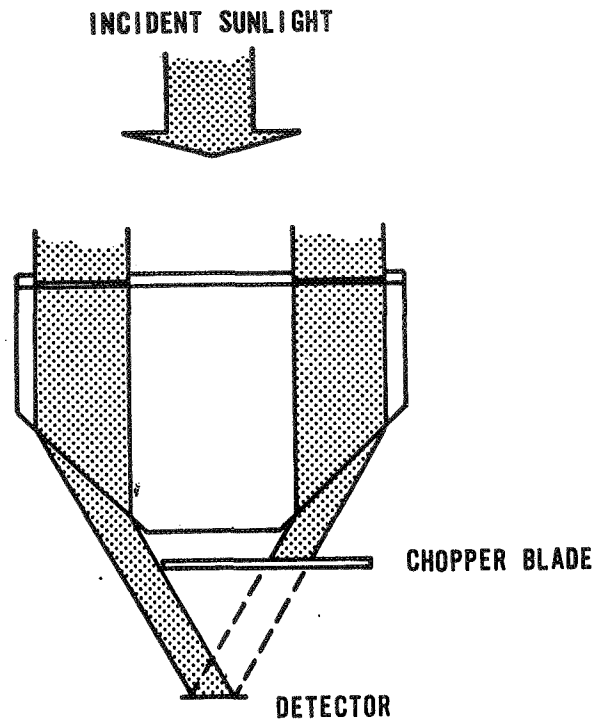
DETECTOR

Figure 22. Chopper blade location.

DETECTOR

DETECTOR MASK

NULL LIGHT
BEAMS

SCALE
0.254 cm

0.190

0.292

RAY 0.75°
OFF AXIS

CHOPPER @ PEAK EXCURSION

CHOPPER AT
REST POSITION

CRITICAL
ANGLE
PRISM

0.635

CAP MASK

0.127
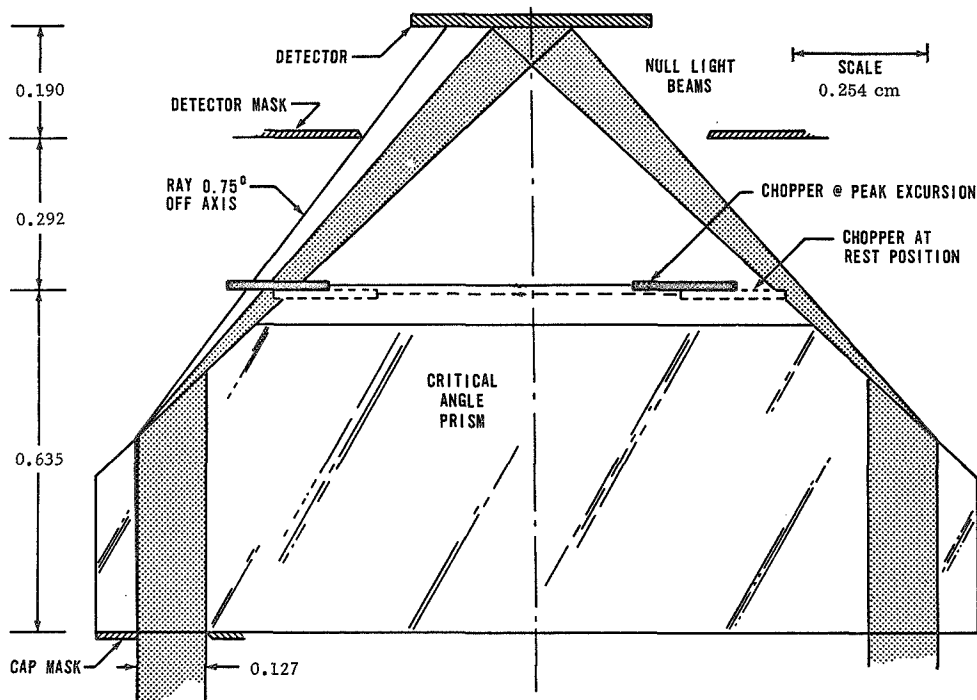
Figure 23. CAP critical dimensions.

32

POLE PIECE

POLE MAGNET

FRAME

BLADE

N

S

N

S

BOLT

COIL
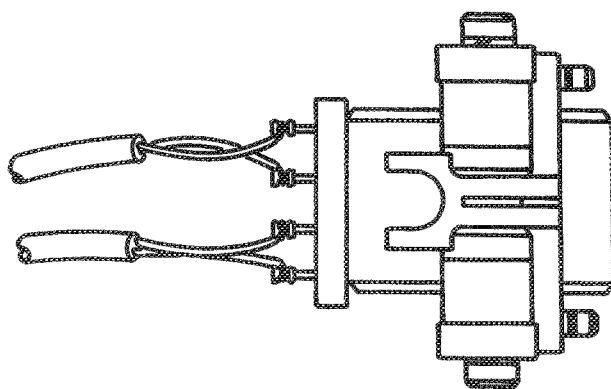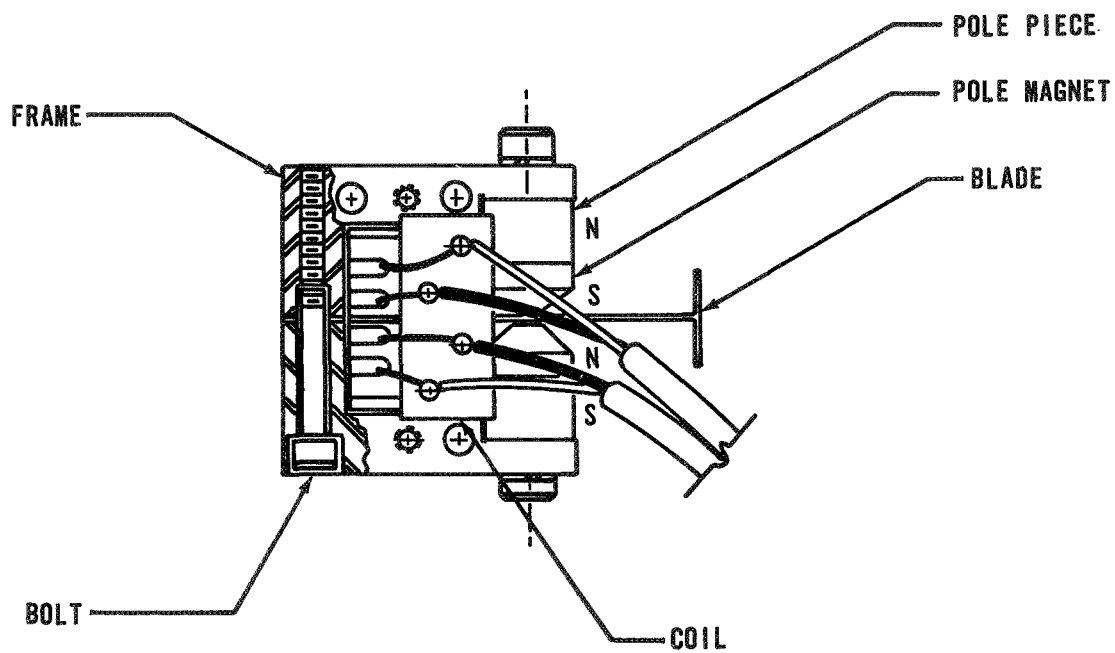
Figure 24. Chopper assembly.
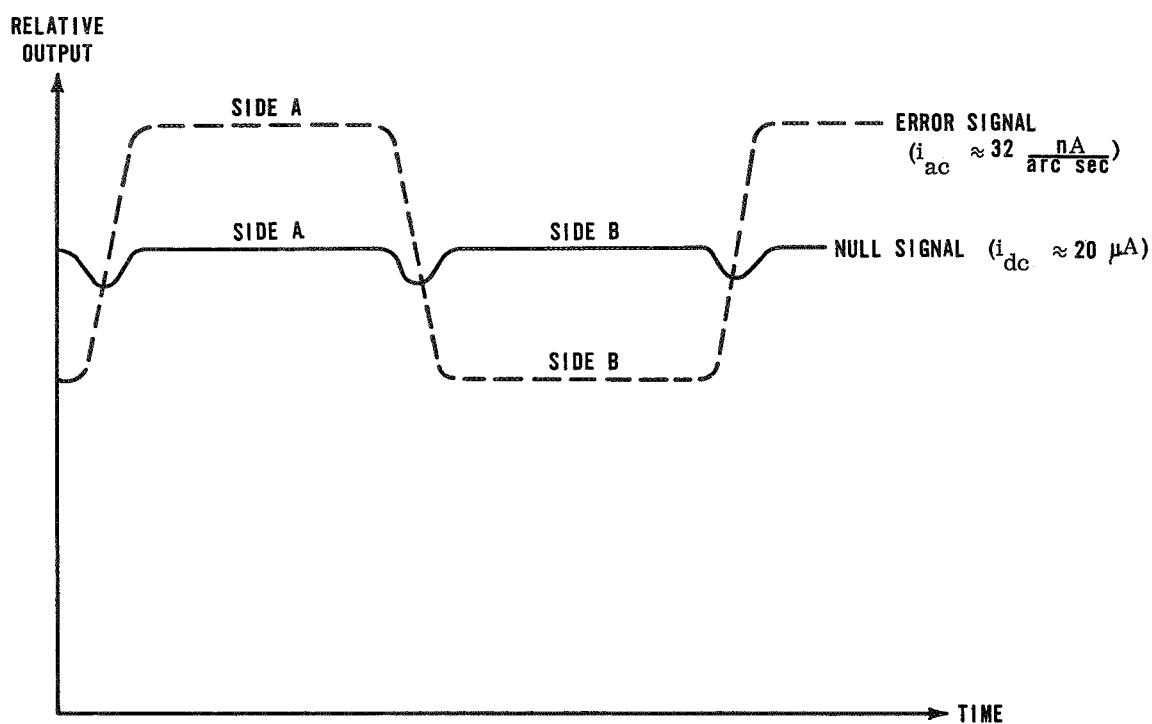
Figure 25. Prism detector waveform.
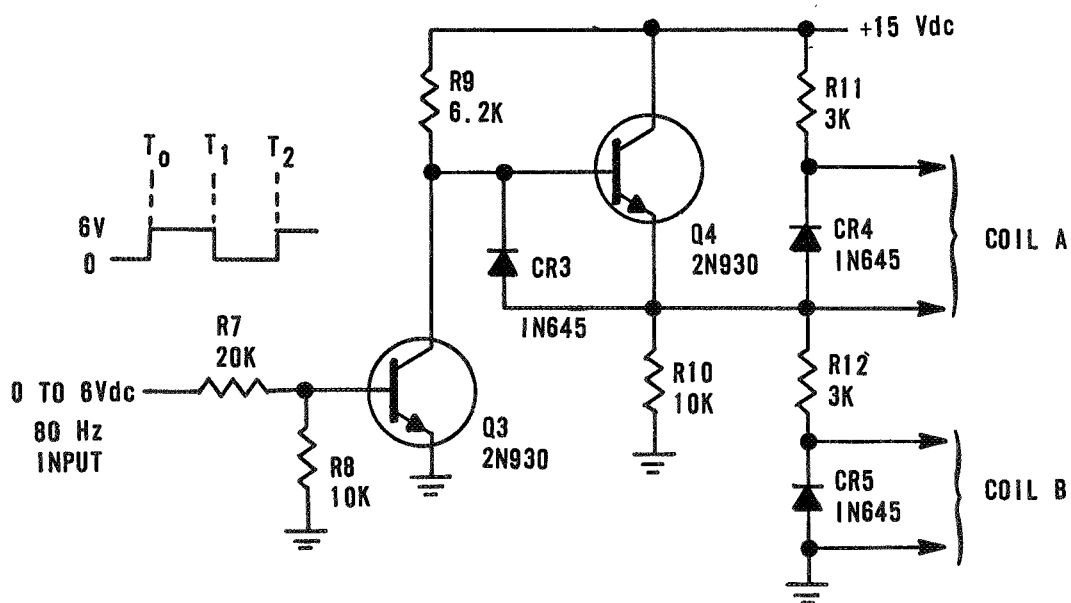
Figure 26. Chopper drive circuit.

Figure 27. CAP electronics block diagram.
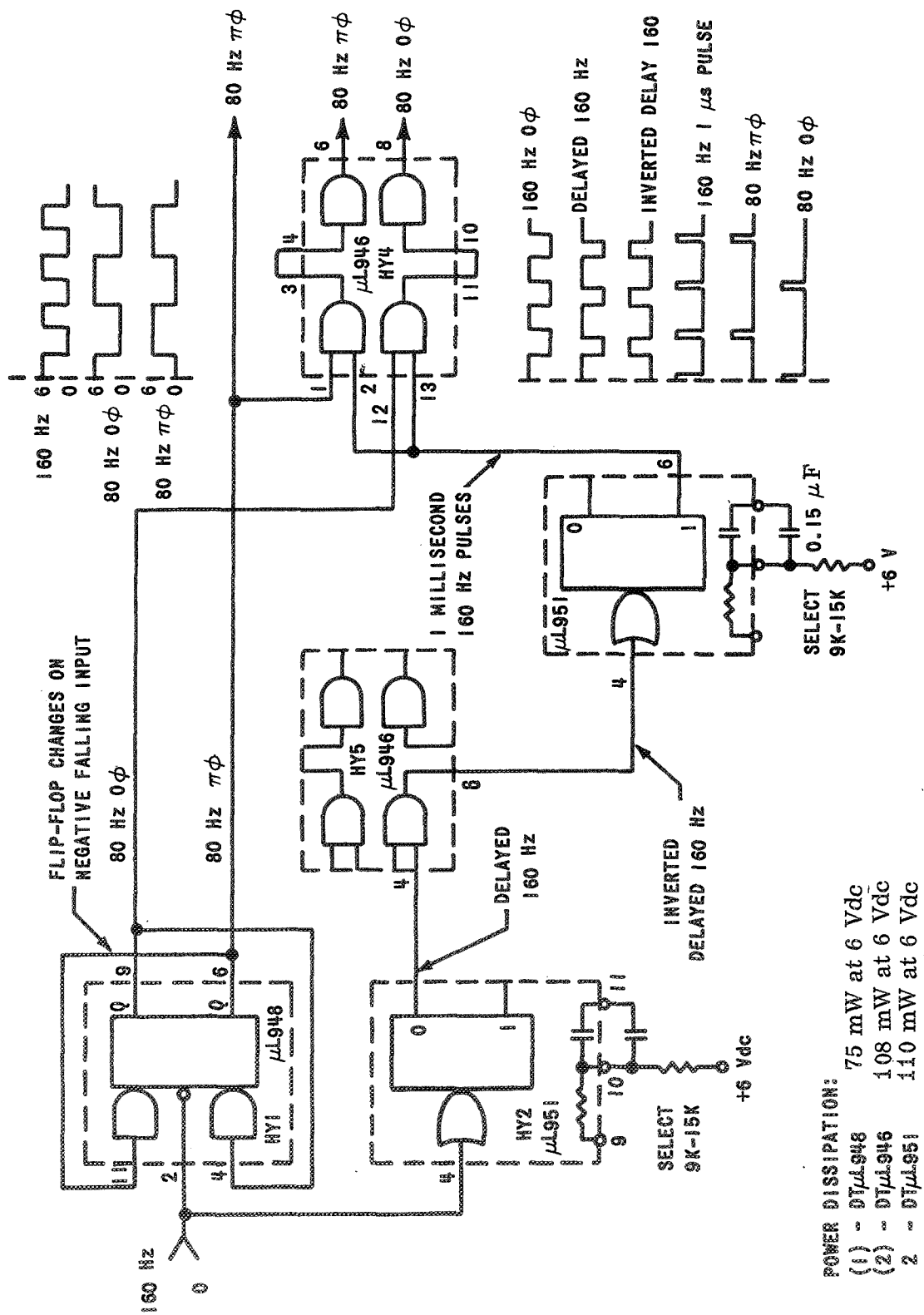
Figure 28. Logic diagram for demodulator reference pulses.

36
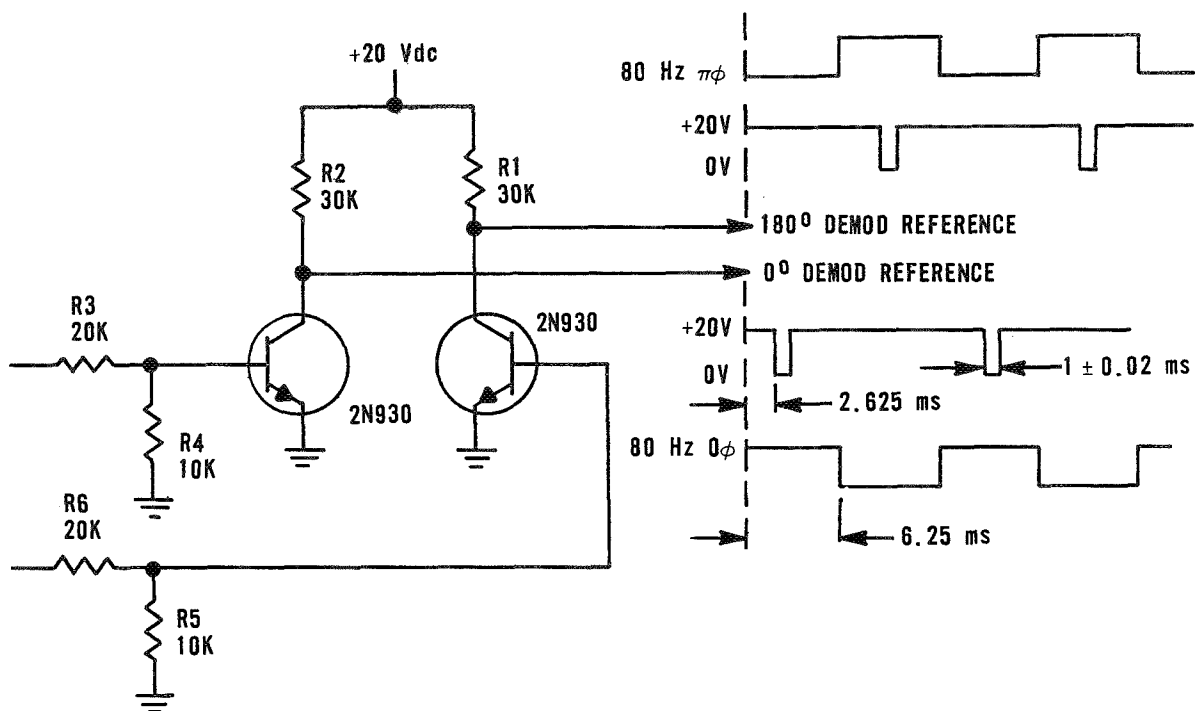
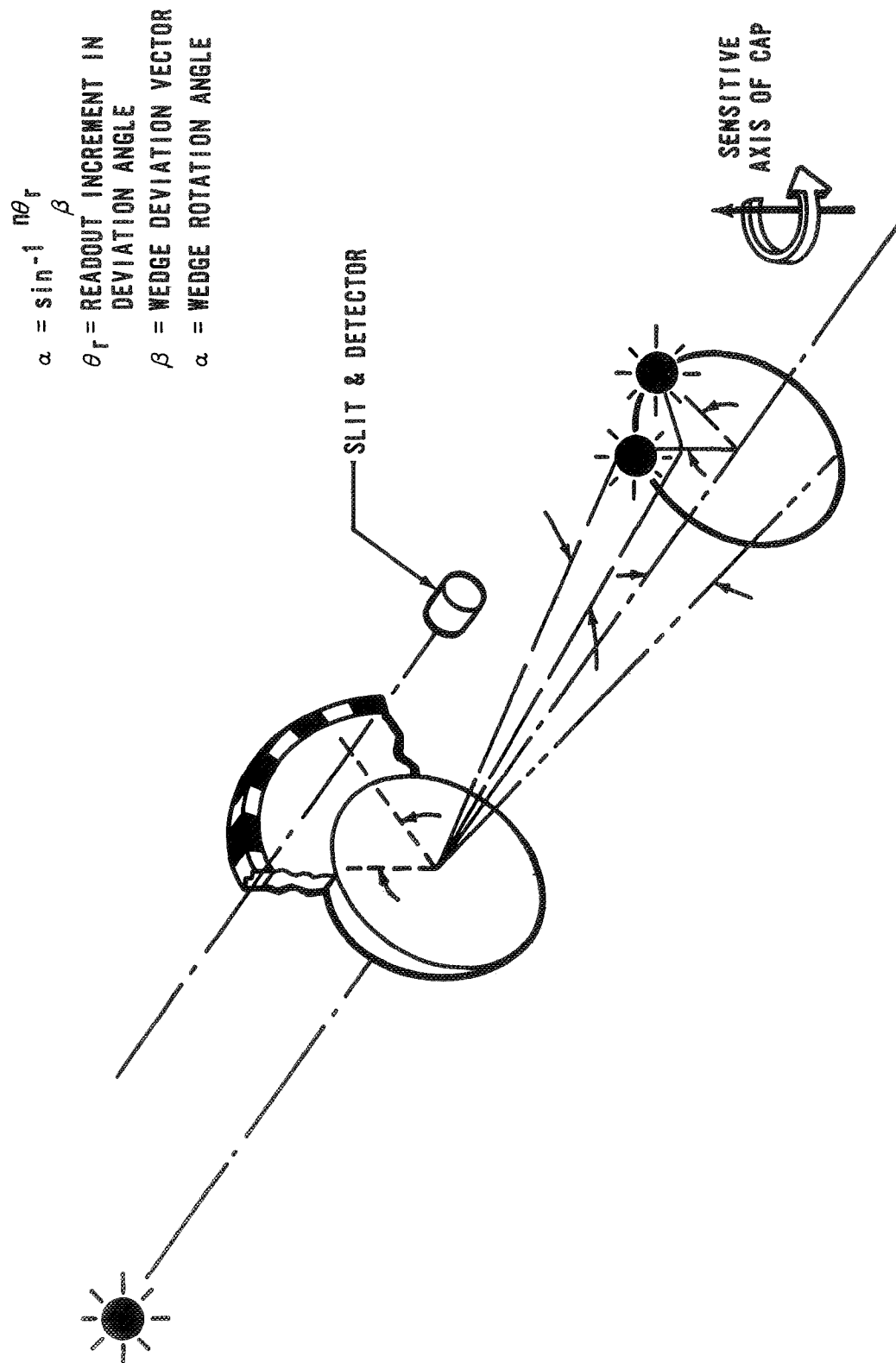Figure 29. Demodulator driver.
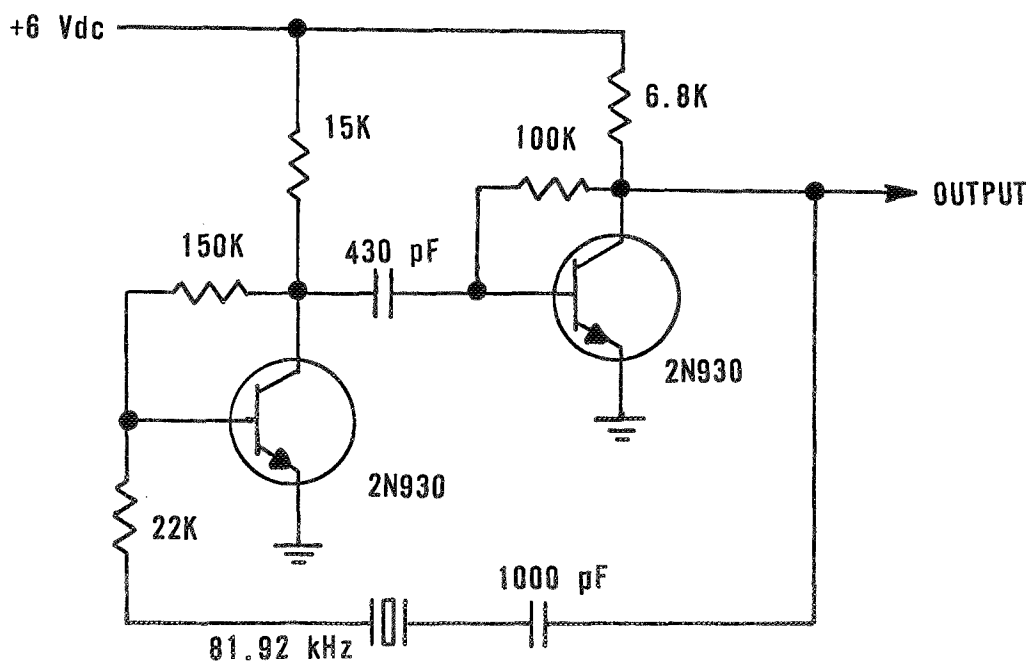
Figure 30. 81.92-kHz oscillator.

$$\alpha = \sin^{-1} \frac{n\theta_r}{\beta}$$

θ_r = READOUT INCREMENT IN DEVIATION ANGLE

β = WEDGE DEVIATION VECTOR

α = WEDGE ROTATION ANGLE

SLIT & DETECTOR

SENSITIVE AXIS OF CAP

Figure 31. ATM-FSS deviation wedge and readout.
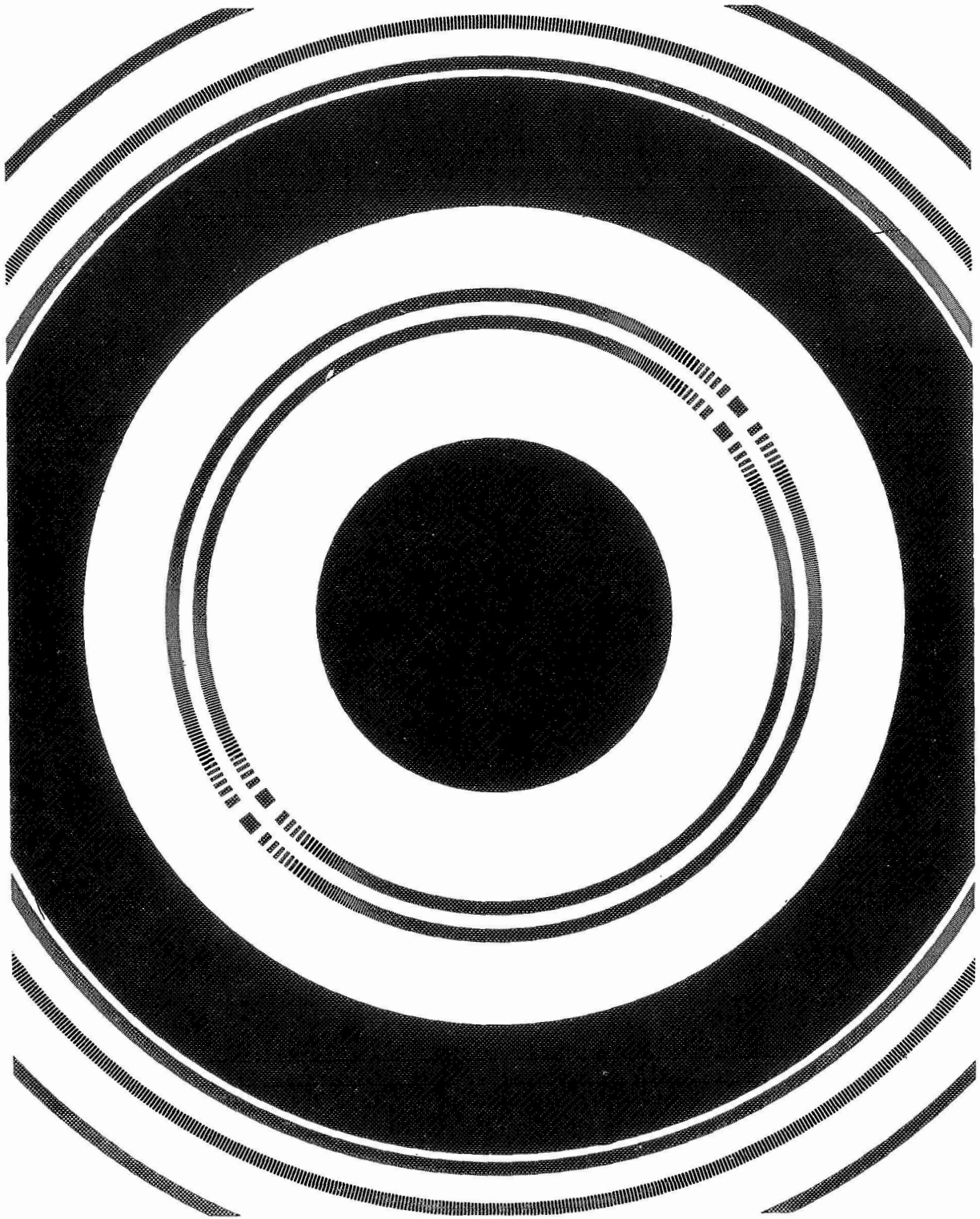
Figure 32. Code pattern.
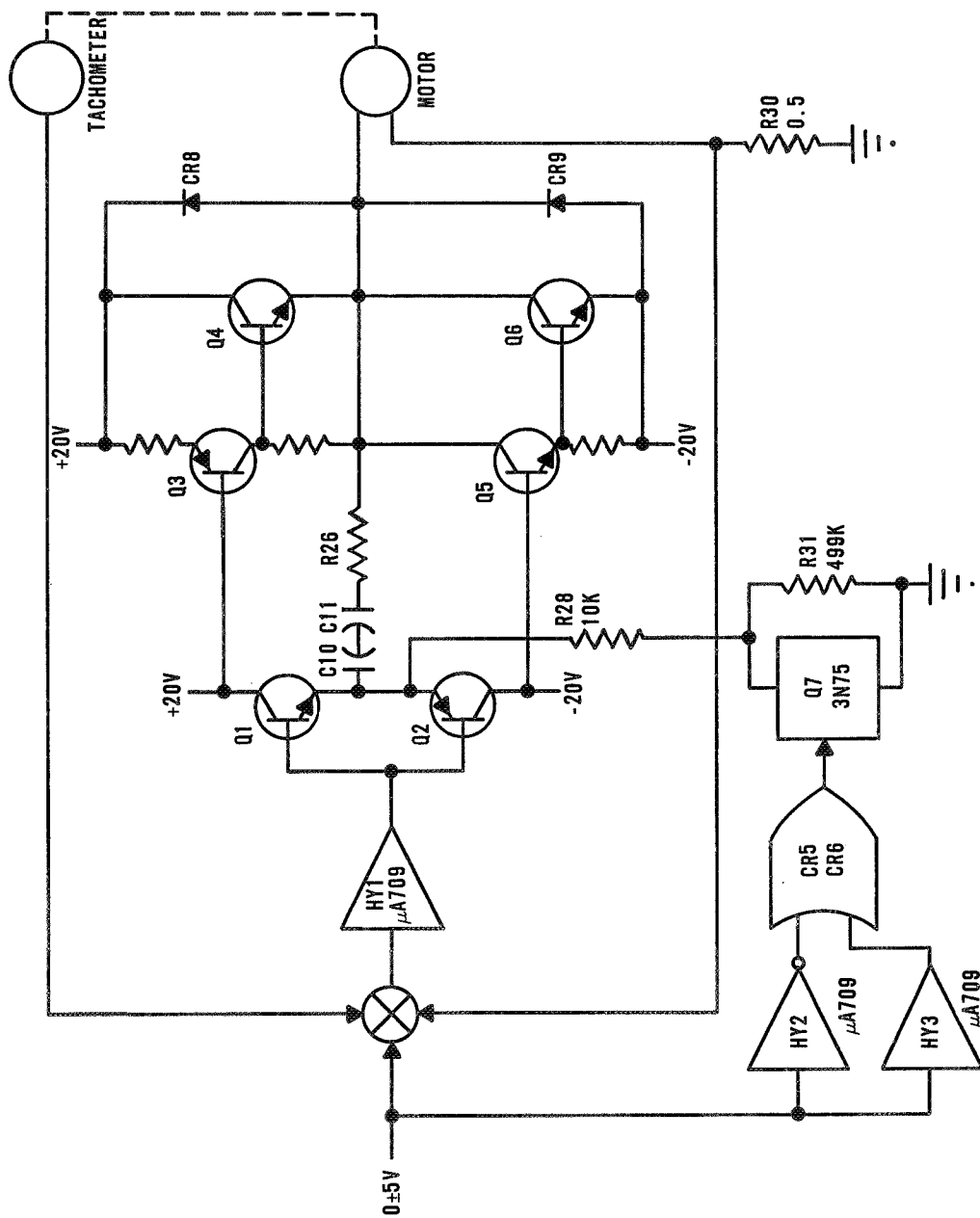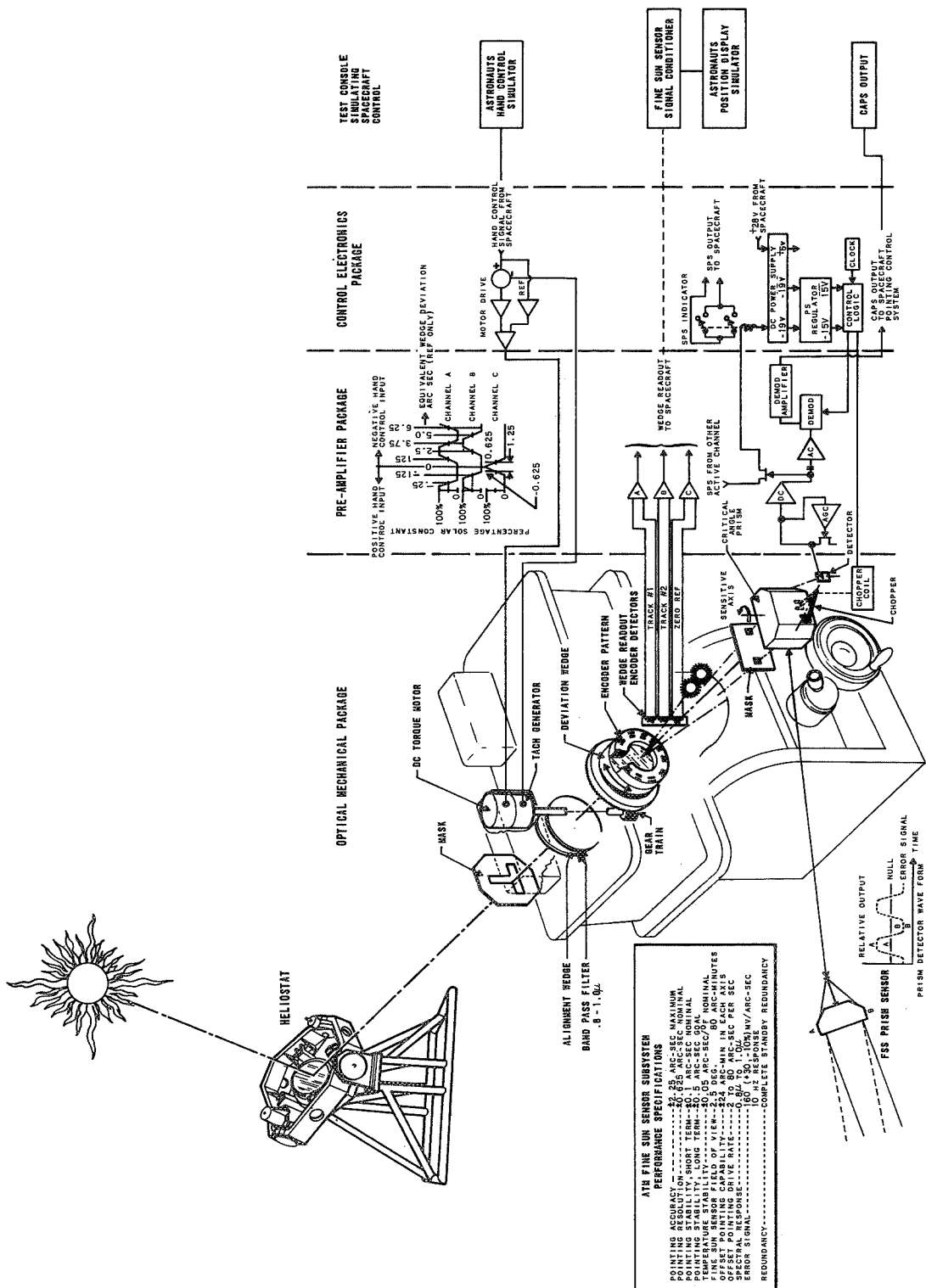
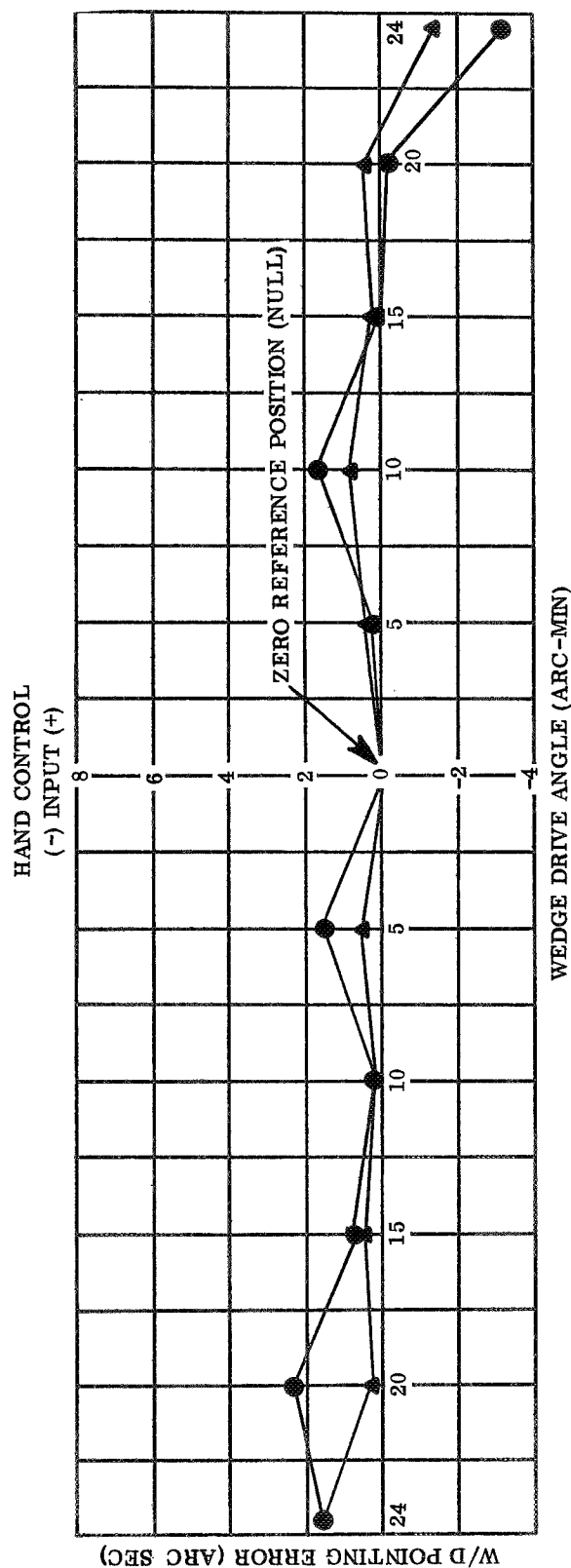Figure 33. Motor control circuit.

40

Figure 34. ATM-FSS pointing accuracy test mode.

41

Figure 35. Typical wedge drive pointing accuracy.
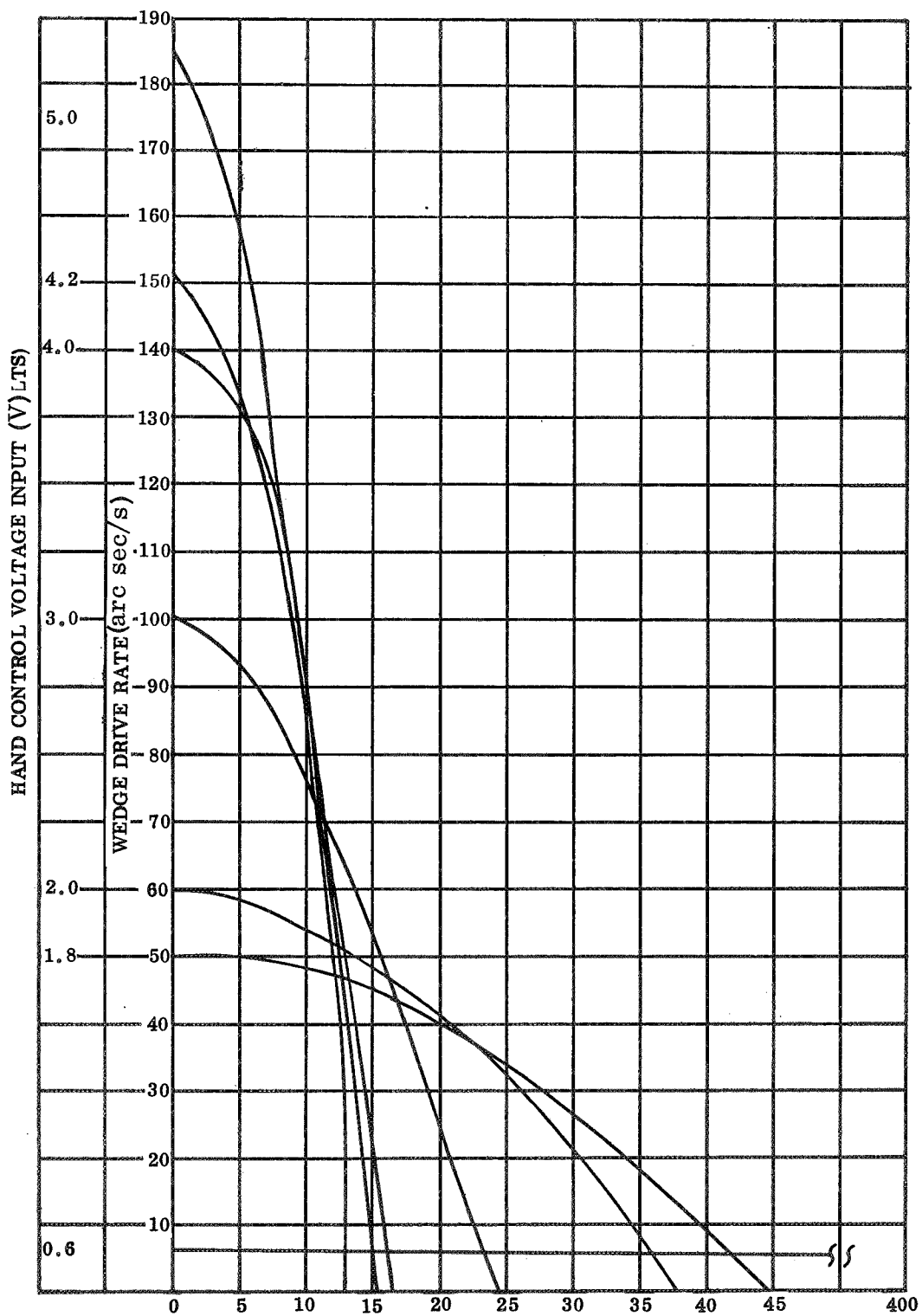
Figure 36. Various drive rates for the ATM-FSS.

A. FSS OM Assembly

1. Vibration Tests (OM)
2. Alignment Check
3. Acceleration Test
4. Alignment Check
5. Acoustical Noise Test
6. Alignment Check
7. Thermal Test
8. Alignment Check

B. FSS PE Assembly

1. Vibration Tests (PE)
2. PE Performance
3. Thermal Shock Test
4. Acceleration Test
5. Thermal Test
6. Acoustical Noise Test
7. PE Performance Test

C. FSS CE Assembly

1. Vibration Tests (CE)
2. CE Performance Test
3. Thermal Shock Test
4. Acceleration Test
5. Thermal Test
6. Acoustical Noise Test
7. CE Performance Test

Phase II: FSS System Tests

A. System Integration
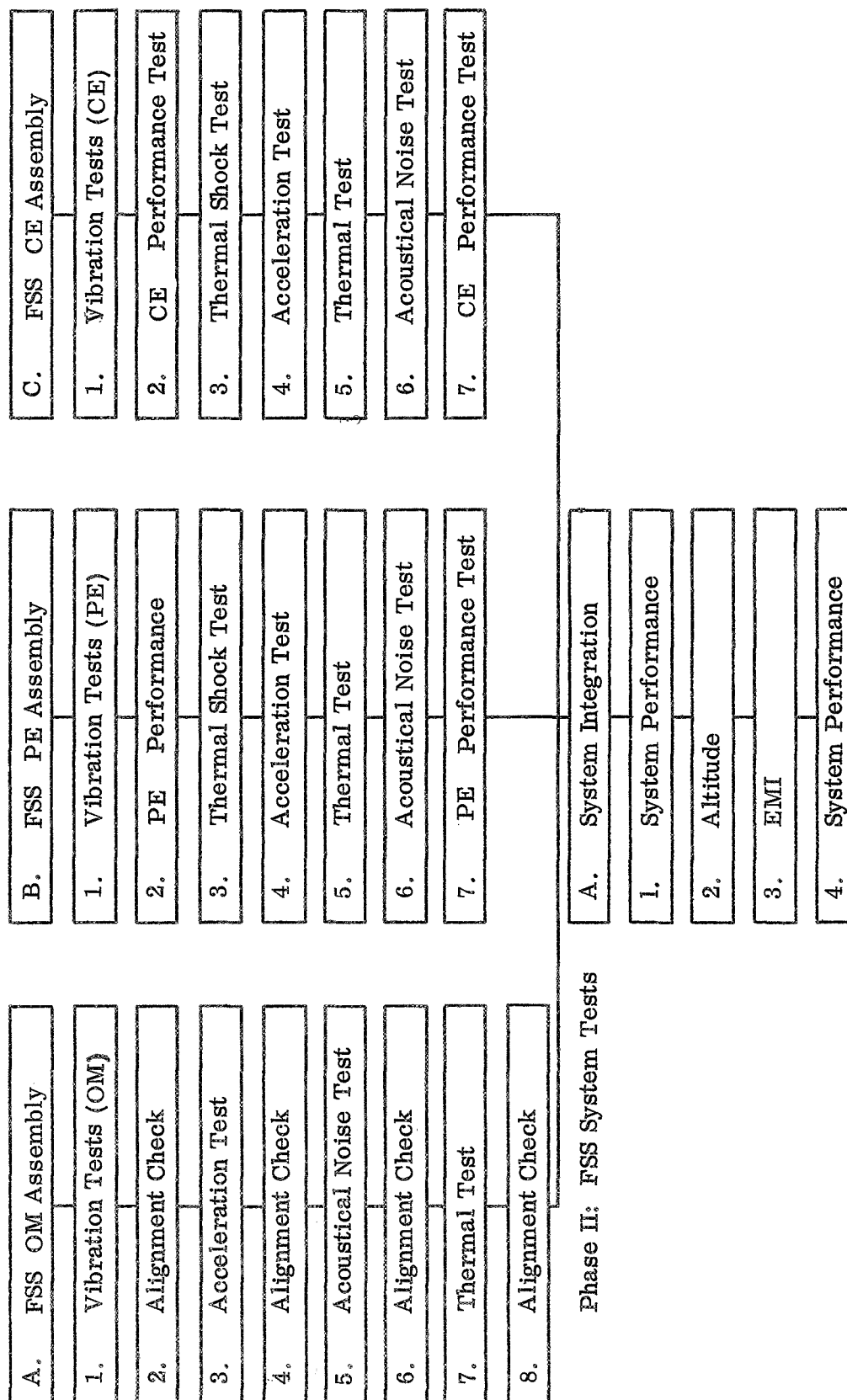
1. System Performance
2. Altitude
3. EMI
4. System Performance

Figure 37. FSS qualification test flow chart.

A FINE SUN SENSOR FOR SKYLAB'S APOLLO
TELESCOPE MOUNT

By J. D. Johnston

The information in this report has been reviewed for security classification. Review of any information concerning Department of Defense or Atomic Energy Commission programs has been made by the MSFC Security Classification Officer. This report, in its entirety, has been determined to be unclassified.

This document has also been reviewed and approved for technical accuracy.

PETER H. BROUSSARD, JR.
Chief, Sensors Branch

CARL H. MANDEL
Chief, Guidance and Control Division

F. B. MOORE
Director, Astrionics Laboratory

INTERNAL

DIR
DEP-T
AD-S
A&TS-MS-H
A&TS-MS-IL (8)
A&TS-MS-IP (2)

PD-AP-DIR
  Mr. Stewart

PD-DO-DIR
  Dr. Thomason

PM-SL (AAP)
  Mr. Ise (3)

PM-PR-M

S&E-DIR
  Mr. Richard

S&E-CSE-DIR
  Dr. Haeussermann

S&E-CSE-A
  Mr. Hagood
  Mr. Hunter

S&E-P-ATM
  Mr. Cagle

S&E-ASTR-DIR
  Mr. Moore
  Mr. Horton

S&E-ASTR-A
  Mr. Hosenthien
  Miss Flowers

S&E-ASTR-B
  Mr. Kampmeier
  Mr. Rowell
  Mr. Spears
  Mr. Ham

S&E-ASTR-C
  Mr. Swearingen

S&E-ASTR-E
  Mr. Aden

S&E-ASTR-G
  Mr. Mandel
  Dr. Doane
  Mr. Wood
  Mr. Jones
  Mr. Doran
  Mr. Broussard
  Mr. Morgan
  Mr. Kelley
  Mr. Lee
  Mr. Kalange
  Mr. Smith
  Mr. Fikes
  Mr. Gaines
  Mr. Walls
  Mr. Johnston (15)

S&E-ASTR-I
  Mr. Duggan

S&E-ASTR-M
  Mr. Boehm
  Mr. Allen

S&E-ASTR-R
  Mr. Taylor

46

S&E-ASTR-S
  Mr. Wojtalik
  Mr. Noel
  Mr. Brooks

A&TS-PAT
  Mr. Wofford

A&TS-TU (6)
  Mr. Winslow

S&E-ASTR-ZX

The Bendix Corporation
Navigation and Control Division
Teterboro, New Jersey 07608
Attn: Mr. H. Schulien
      Mr. B. Ficken
      Mr. R. Abramowitz

EXTERNAL

Scientific and Technical Information Facility (25)
P. O. Box 33
College Park, Maryland 20740
Attn: NASA Representative (S-AK/RKT)

National Aeronautics and Space
  Administration
Washington, D. C. 20546
Attn: Mr. Theordore Michaels, REG
      Mr. Authur Reetz, Jr., RX
      Mr. Richard Livingston, MTG
      Mr. Carl Janow, REG
      Mr. William Hamby, HLO

Langley Research Center
National Aeronautics and Space
  Administration
Langley Station
Hampton, Virginia 23365
Attn: Dr. Kurzhals (5)
      Mr. Keckler (5)